Dear Prof. Yu (Editor):

We are submitting a second revision of our paper entitled, "Long-term air concentrations, wet deposition, and scavenging ratios of inorganic ions, HNO_3 and SO_2 and assessment of aerosol and precipitation acidity at Canadian rural locations", for potential publication in Atmospheric Chemistry and Physics. We have addressed all the additional comments provided by reviewer 1 on our revised manuscript. Please see enclosed responses and track changes version of the paper.

Thank you for taking care of the review process.

Sincerely,

Irene Cheng and Leiming Zhang

Air Quality Research Division
Environment and Climate Change Canada

Response to Reviewer 1 – Second Review

I have read the revised version of the manuscript in detail and with great interest. I greatly appreciate the authors making the effort to address reviewer comments. I believe that the manuscript is now much strengthened and readable. Below I have listed some comments, which in my opinion still require some attention.

We appreciate the additional detailed comments that this reviewer provided to further improve and condense the materials in our paper. Our responses to the comments are provided below.

Specific comments

Both in the abstract and the text it is stated that the study analyzed long-term air concentrations, wet deposition, and precipitation acidity at 30 Canadian sites. The list of sites in Table 1, and Figure 6 and 8, however, include a total of up to 31 sites. Figure S1 shows the location of 29 sites only. These discrepancies are probably because of the duplicate stations in Egbert and Goose Bay, so, is 31 the final number of sites? If so please correct that number in the abstract, in the caption of Figure S1, and throughout the text.

Response: There are 31 sites; however there are two sets of precipitation concentrations at Egbert that are co-located. Thus, we stated there were actually 30 sites. Note that the two Goose Bay measurements are not exactly co-located as indicated by the slight differences in the geographical coordinates in Table 1. To ensure the number of sites is consistent, we changed the number of sites to 31 (now including the co-located measurement at Egbert) and added Egbert-2 and Goose Bay B to the map in Fig. S1.

Furthermore, differences in the availability of measurements among sites and years limited the comparison of results to a shorter number of locations (those with more than 9 years of data). As a result, the data presented in figures and tables, as well as the calculated averages, ranges, and trends mentioned and compared throughout the text, do not include results from all 31 locations in a consistent manner. For example, 16 sites were used for rates of change in annual air concentration/wet deposition data shown in tables 1, 2, and 3, while 12-14 sites were used for geographical patterns in air concentrations in figure 1, or 31 sites for wet deposition in figure 6. I imagine that for those same problems with data availability, the X axes of left and right panels in Figure 1 do not correspond to the same stations. Cree Lake and Montmorency data is shown only in 1983-1996 panels, while Bratt's Lake, Sprucedale, Frelighsburg, and Lac Edouard data appear in 1997-2010 panels only. Please summarize in the methods section the number of stations and/or time period used for each of the analyses on each of the subsections, as well as clarify the number of sites used for the calculation of averages and ranges presented in the text.

Response: This information has been provided in the paper already. In sect. 2.1.2 of the Methods section, we mentioned that air concentrations were available at 16 sites. In sect. 2.1.3, we mentioned that precipitation concentrations were available at 30 sites (two co-located collectors at Egbert). Note the change to 31 sites in the revised paper. Also in section 2.1.1, we stated that the measurement periods are not synchronized between all sites with some sites having different start and end dates. The data coverages for each site were provided in Table 1.

I am still not comfortable with the correlation analyses carried out between meteorological variables and particulate ions and trace gas data presented in page 10 (lines 14 to 34). I do not think that monthly averaged data correlations (or lack of) provide much information about the influences of temperature, precipitation, or relative humidity on observed K+ and NH4+ long-term trends. The use of Pearson correlation coefficients based on monthly averages to explain the long-term trends based on annual values seems a priori not very convincing. This is a complicated issue, as we are dealing with substances that differ in nature, origin, chemistry, and interactions with other pollutants. There is much evidence that current and future climatic variability and trends modulate the magnitude of annual emissions for substances like ammonia (Sutton et al. 2013). It is possible that Pearson correlation analysis of monthly data was not the best choice here. Considering that these analyses do not contribute much to the overall manuscript focus and goals, nor essential to support authors' main conclusions, I would suggest to eliminate these paragraphs in the final version of the manuscript. If necessary to support some of the statements authors made, reader can always be referred to the supplementary data. Doing so authors might improve clarity and it will also help reduce the sometimes "overwhelming" amount of data presented in the text, a concern that I expressed in my first round of comments.

Response: This paragraph has been moved to sect. S1 of the Supplementary Material which supports the time-series graphs (Fig. S2) and the correlation analysis results (Table S1) that were already in the supplement. The last sentences of sect. S1 have been revised based on the reviewer's comments and the references by Sutton et al. (2013) and Yao and Zhang (2016). Sutton et al. (2013) suggests an increase in temperature by a few degrees would increase ammonia emissions. Yao and Zhang (2016) also suggest increasing ammonia emission with increasing temperature and provided two mechanisms: (1) ammonia emissions from soil would increase with increasing temperature, and (2) an increase in temperature would increase ammonium nitrate partitioning to gas-phase ammonia. Yao and Zhang (2016) further pointed out that the simultaneous decrease in sulfur dioxide emissions would likely reduce atmospheric sulfate and subsequently lead to lower ammonium sulfate. Thus, there are uncertainties on the effects of meteorological variables like temperature on the long-term sulfate and ammonium trends. The last sentences now reads, "The correlation analysis using monthly data did not find a strong relationship between long-term temperature changes and long-term trends in SO_4^{2-} and NH_4^+ concentrations. The lack of trends is related to the combined effects of increasing temperature and decreasing sulfur dioxide emissions. Studies suggest an increase in temperature would increase ammonia emissions and the partitioning of ammonium nitrate to ammonia (Sutton et al., 2013; Yao and Zhang, 2016). However, the decreasing trend in sulfur dioxide emissions would likely reduce atmospheric sulfate and subsequently lead to lower ammonium sulfate production (Yao and Zhang, 2016)."

Additional comments

Page 5, line 22: What do authors mean by "insufficient data"? Please clarify.

Response: To clarify, we revised the sentence to, "If there is insufficient data (<15 daily measurements) in each month, the scavenging ratio is not calculated."

Page 7, line 10; Page 8, line 4; and elsewhere: authors refer to Fig. 1a and 1b while there are no such a and b panels, or they have not been labeled. Maybe left and right?

Response: The labeling of the part a and b figure is incorrect. Figure 1 has been revised. There are no longer part a and b panels in the revised figure.

Figure 1: a 3-page figure seems a bit excessive. First, many of the elements should be deleted. Y-axis title (air concentration ug m-3) is the same for all panels so it can be placed just once, centered on the left. Y-axis tick labels and scale are identical between left and right panels so they do not need to be present on the right panel axis. X-axis labels are the same for the different substances so they only need to be shown on the bottom panel X-axes. Ion/trace gas labels only need to be shown in one of the two panels and not both. These adjustments will reduce the size of figure 1. Second, as a suggestion, authors might want to consider combining both panels in one single graph per substance, showing boxes of different colors (one color for 1983-1996 and another color for 1997-2010, stations that have data for one period only will show one box only).

Response: We revised the graphs according to both your suggestions. The figure has been condensed to 1 page. The white box graph is for the 1983-1996 data and the green box graph is for the 1997-2010 data (site labels also shown in green for this period).

Figure 6: As said for figure 1, please allocate X-axis labels on the bottom panel only, and just one Y-axis title centered.

Response: Revised according to your suggestions. The figure has been condensed to 1 page.

References cited

Sutton, M. A., S. Reis, S. N. Riddick, U. Dragosits, E. Nemitz, M. R. Theobald, Y. S. Tang, C. F. Braban, M. Vieno, A. J. Dore, R. F. Mitchell, S. Wanless, F. Daunt, D. Fowler, T. D. Blackall, C. Milford, C. R. Flechard, B. Loubet, R. Massad, P. Cellier, E. Personne, P. F. Coheur, L. Clarisse, M. Van Damme, Y. Ngadi, C. Clerbaux, C. A. Skjøth, C. Geels, O. Hertel, R. J.

Wichink Kruit, R. W. Pinder, J. O. Bash, J. T. Walker, D. Simpson, L. Horváth, T. H. Misselbrook, A. Bleeker, F. Dentener, and W. de Vries. 2013. Towards a climate-dependent paradigm of ammonia emission and deposition. Philosophical transactions of the Royal Society of London. Series B, Biological sciences 368:20130166.

Yao, X. and Zhang, L.: Trends in atmospheric ammonia at urban, rural, and remote sites across North America, Atmos. Chem. Phys., 16, 11465-11475, doi:10.5194/acp-16-11465-2016, 2016.

Long-term air concentrations, wet deposition, and scavenging ratios of inorganic ions, HNO_3 and SO_2 and assessment of aerosol and precipitation acidity at Canadian rural locations

Irene Cheng and Leiming Zhang

Air Quality Research Division, Science and Technology Branch, Environment and Climate Change Canada, 4905 Dufferin Street, Toronto, Ontario, M3H 5T4, Canada

Correspondence to: Irene Cheng (irene.cheng@canada.ca)

Abstract. This study analyzed long-term air concentrations and annual wet deposition of inorganic ions and aerosol and precipitation acidity at ~~30~~ 31 Canadian sites from 1983-2011. Scavenging ratios of inorganic ions and relative contributions of particulate- and gas-phase species to NH_4^+, NO_3^-, and SO_4^{2-} wet deposition were determined. Geographical patterns of atmospheric Ca^{2+}, Na^+, Cl^-, NH_4^+, NO_3^-, and SO_4^{2-} were similar to wet deposition and attributed to anthropogenic sources, sea-salt emissions, and agricultural emissions. Decreasing trends in atmospheric NH_4^+ (1994-2010) and SO_4^{2-} (1983-2010) were prevalent. Atmospheric NO_3^- increased prior to 2001 and then declined afterwards. These results are consistent with SO_2, NO_x and NH_3 emission trends in Canada and the U.S. Widespread declines in annual NO_3^- and SO_4^{2-} wet deposition ranged from 0.07-1.0 kg ha^{-1} a^{-1} (1984-2011). Acidic aerosols and precipitation impacted southern and eastern Canada more than western Canada; however both trends have been decreasing since 1994. Scavenging ratios of particulate NH_4^+, SO_4^{2-} and NO_3^- differed from literature values by 22%, 44% and a factor of 6, respectively, because of the exclusion of gas scavenging in previous studies. Average gas and particle scavenging contributions to total wet deposition were estimated to be 72% for HNO_3 and 28% for particulate NO_3^-, 37% for SO_2 and 63% for particulate SO_4^{2-}, and 30% for NH_3 and 70% for particulate NH_4^+.

1 Introduction

The Canadian Air and Precipitation Monitoring Network (CAPMoN) measures trace gas concentrations and particulate inorganic ion concentrations in air and precipitation at rural locations across Canada. Since 1983, the network has been collecting filter and precipitation samples and the number of sites has expanded to 33 as of 2010. CAPMoN was developed to monitor trends in atmospheric pollutants contributing to smog and acid rain, and the data was later used to assess the impacts of environmental policies in the Canada-U.S. Air Quality Agreement. This bilateral agreement signed in 1991 recognizes the impacts of transboundary pollution and sets objectives to reduce SO_2 and NO_x emissions.

In this study, the focus is on the particulate base cations (Ca^{2+}, Mg^{2+}, K^+, Na^+, NH_4^+) and acidic anions (Cl^-, NO_3^-, and SO_4^{2-}), nitric acid, and sulfur dioxide that have direct impacts on acid rain. Nitrates and sulfates in acid rain reduce soil quality by causing the depletion of base cations, which are plant nutrients and are also involved in neutralizing acids. Base cations in soil can be replenished by mineral weathering, deposition, wind erosion, agricultural tilling, and forest fires (Hedin et al., 1994; Driscoll et al., 2001). However, when acidic deposition exceeds the supply of base cations, soil acidification occurs. Soil acidity has consequently increased the leaching of inorganic aluminum (Al) monomers, which is a toxic form of Al to plants and animals (Driscoll et al., 2001). Trees (e.g., red spruces and sugar maples) experienced damage to foliage, decreased adaptability to cold climates, slower growth, and mortality during 1960s-1980s from direct and indirect impacts of acid rain (Driscoll et al., 2001; Watmough and Dillon, 2003). Acid rain and runoff of acidic soil also increased nitrates, sulfates and inorganic Al and reduced pH in surface waters of Atlantic Canada, southcentral Ontario, and northeastern U.S. (Clair et al., 2002; Driscoll et al., 2003; Jeffries et al., 2003). Lake acidification has led to detrimental effects including mortality on zooplankton and fish (Driscoll et al., 2001 and references therein). Terrestrial birds are also impacted because when calcium is depleted from soil, less calcium-rich insects are available for birds to consume (Hames et al., 2002). Calcium deficiency in birds can cause eggshell thinning and other reproductive consequences (Hames et al., 2002).

Assessments of lake acidification in the previous decade indicate declines in nitrates and sulfates in surface water, some improvements to pH and acid neutralizing capacity, and conversion to less toxic organic Al (Clair et al., 2002; Driscoll et al., 2003; Jeffries et al., 2003; Kothawala et al., 2011; Strock et al., 2014). Although nitrate and sulfate deposition have been decreasing, surface water conditions have not improved at the same rate because nitrates and sulfates that have accumulated in soil and wetlands over a long period of time is gradually releasing to surface waters (Stoddard et al., 1999; Driscoll et al., 2001; Clair et al., 2002; Jeffries et al., 2003). A recent assessment by Lawrence et al. (2015) indicates no additional soil acidification and that acid deposition effects on soil have started to diminish in northeastern U.S. and eastern Canada according to indicators, such as exchangeable Ca and Al, base cations, and pH levels. Considering the role of inorganic ions on acid deposition effects on biota, it is important to continually study the wet deposition of inorganic ions.

The wet deposition of particulate base cations and acidic anions depend on the particulate concentrations of these inorganic ions in air and some trace gases, such as nitric acid and sulfur dioxide. This simplified relationship is the premise behind the scavenging ratio, defined as a ratio of a pollutant's concentration in precipitation to that in air. In reality, wet deposition is a very complex process that involves an understanding of cloud and precipitation processes and aqueous phase chemistry, which are considered to be the major sources of uncertainty in wet deposition modeling (Tost et al., 2007; Kajino and Aikawa, 2015). Scavenging ratios can be considered a measure of the wet scavenging efficiency of air pollutants, since they have been used to compare the precipitation removal of different pollutants in previous studies (Galloway et al., 1993; Guerzoni et al., 1995; Tuncel and Ungör, 1996; Shrestha et al., 2002; Hicks et al., 2005; Kulshrestha et al., 2009; Bourcier et al., 2012; Zhang et al., 2015). These studies demonstrated that scavenging ratios vary according to particle size distribution similar to the particle size dependency of scavenging coefficients typically used in wet deposition modeling (Wang et al., 2014). Thus, scavenging ratios of particulate-phase pollutants have been used as a surrogate for other particulate-phase pollutants with similar particle sizes (Cadle et al., 1990; Sakata and Asakura, 2007; Cheng et al., 2015).

The objectives of this study were to (1) analyze long-term geographical patterns and temporal trends in nitric acid and sulfur dioxide concentrations and the air concentrations and wet deposition of base cations and acidic anions; (2) examine geographical and temporal trends in aerosol acidity and acid rain; (3) determine scavenging ratios for particulate inorganic ions using precipitation and air concentrations; and (4) develop an approach for estimating particulate and gaseous species wet scavenging contributions to total nitrate, ammonium and sulfate wet deposition and their scavenging ratios.

2 Methodology

2.1 Data description

2.1.1 CAPMoN datasets

24-hr integrated trace gas concentrations and particulate inorganic ion concentrations in air and precipitation are measured by CAPMoN at rural locations across Canada. This dataset was accessed online from the NAtChem database (Environment Canada, 2015a). The monitoring sites are located in various regions of Canada with the majority of the sites residing in the province of Ontario and Quebec (Fig. S1). Site elevations range from 14-707 m.a.s.l. The sites include continental and coastal sites, and the land use types of most CAPMoN sites are categorized as forested or agricultural sites (Table 1). Only the sites with long-term data (≥9 years) were analyzed in this study. The measurement periods are not synchronized between all sites; therefore, some sites may have different starting and end dates.

2.1.2 Air concentrations

Non-size selective filters are used to collect air samples, which are analyzed for major inorganic ions (Ca^{2+}, Mg^{2+}, K^+, Na^+, Cl^-, NH_4^+, NO_3^-, and SO_4^{2-}) and HNO_3 and SO_2 trace gases. Teflon filters are used for the inorganic ions, while nylon and impregnated cellulose filters are used for HNO_3 and SO_2, respectively. The filters are placed in a three stage filter pack, which samples air at 10 m above ground. Every 24 hr at 8:00 LT, the sequential sampler passes air through a different filter pack. The filters are retrieved and delivered to CAPMoN laboratories for chemical analysis. The collected mass for each species, blank values, and mass flow rates are used to determine the air concentrations in μg m^{-3}. Quality control of the data are performed using the Research Data Management and Quality Assurance System (RDMQ™) software (McMillan et al., 2000), which processes and manages large amounts of data, applies quality control checks, and assigns validity flags to each data point. The standard data flags warn users of missing values, invalidated values, valid values below detection limit, valid estimated and interpolated values, non-conforming sampling periods, and valid values that have been replaced by the detection limit. In this study, valid air concentrations from 16 sites were analyzed. Available air measurements between 1983 and 2010 at the 16 sites are shown in Table 1.

2.1.3 Precipitation concentrations

Precipitation is sampled using a wet-only precipitation collector, which automatically opens when sensors detect precipitation. Precipitation is collected in a specially-designed plastic bag in the collector. The bags containing precipitation are retrieved each day between 8:00 and 9:00 LT and are sealed, weighed and then kept refrigerated. The 24-hr integrated precipitation samples are analyzed for H^+ and major inorganic ions (described in Sect. 2.1.2) in concentrations of mg l^{-1}. Precipitation amount is also recorded daily at the precipitation monitoring sites for the determination of wet deposition flux. Standard data flags similar to the air data are applied to the precipitation data. In this study, valid precipitation concentrations from ~~30~~ 31 sites were analyzed. Available precipitation measurements between 1984 and 2011 at the ~~30~~ 31 sites (two collocated collectors at Egbert) are shown in Table 1.

2.1.4 Meteorological data

Hourly air temperature, relative humidity and wind direction data at collocated or nearby stations to CAPMoN sites were obtained from the Canadian Climate Data Archives (Environment Canada, 2015b). Hourly air temperature and relative humidity were averaged to daily values to correspond with the sampling intervals of the air and precipitation concentrations. Hourly wind direction data were used to determine the prevailing wind directions at each site.

2.2. Data analysis

2.2.1 Long-term patterns

Geographical patterns and temporal trends in air concentrations and wet deposition were examined. The geographical patterns in air concentrations were based on 24-hr integrated measurements. For wet deposition, geographical patterns in the annual wet deposition flux were analyzed since annual wet deposition is typically reported in previous studies. Daily precipitation concentrations were multiplied by the corresponding daily precipitation amount above the rain gauge detection limit of 0.2 mm. The annual wet deposition flux was obtained by summing the daily wet deposition flux. Thus, only the years with complete wet deposition data are used to determine the annual wet deposition. Statistical analyses of temporal trends were performed using regression analysis of the annual average air concentrations and annual wet deposition for all years with complete data. The Mann-Kendall Test and Seasonal Kendall Test were also applied to the annual wet deposition and annual average air concentrations, respectively, to assess whether there was a statistically significant monotonic trend (Gilbert, 1987; Prestbo and Gay, 2009; Zbieranowski and Aherne, 2011; Cole et al., 2014). The Seasonal Kendall and Sen's estimator of slope provides the magnitude of the temporal trend on a per year basis. The Seasonal Kendall test analyzes the temporal trend in the average air concentrations in each month separately and then aggregates the results to obtain the annual trend. The Mann-Kendall test was used to obtain the annual total wet deposition trend. Correlation analysis was performed between monthly averaged meteorological parameters and particulate ions and trace gases. For wet deposition of inorganic ions, the correlations with the precipitation amount and air concentrations were examined.

2.2.2 Aerosol acidity

The molar cation/anion charge equivalent ratio (c/a) (Hennigan et al., 2015) was used as a measure of H^+ and aerosol acidity for the air sampling sites. The ions associated with acidic aerosols are predominantly SO_4^{2-} and NO_3^-; however there are also contributions from organic acids which have not been accounted for by the c/a (Kerminen et al., 2001). Base cations and NH_4^+ are involved in neutralizing acidic aerosols. A c/a near 1 indicates that the aerosols are generally neutral, whereas a lower ratio near 0.75 is indicative of acidic aerosols (Zhang et al., 2007; He et al., 2012). Daily c/a were determined only if all the ion measurements are available.

2.2.3 Scavenging ratio

In this study, monthly scavenging ratios (W) were first determined for ions existing only in the particulate phase (Ca^{2+}, Mg^{2+}, K^+, Na^+, and Cl^-) using Eq. 1 (Kasper-Giebl et al., 1998; He and Balasubramanian, 2008):

$$W = \frac{C_{prec}}{C_{air}} \times \frac{\rho_a}{\rho_w}, \quad (1)$$

C_{prec} and C_{air} are the precipitation and air concentrations, respectively. Surface air concentrations were used, even though in theory most of the scavenging occurs at the cloud height (Duce et al., 1991). ρ_a and ρ_w are the densities of air (1.2 kg m^{-3}) and water, respectively, which are used to convert the scavenging ratios to a mass basis. Scavenging ratios were determined on a monthly basis because they have less variability compared to daily (i.e. paired) or precipitation event scavenging ratios (Galloway et al., 1993) and consider the average air concentration during both precipitation and dry periods (Kasper-Giebl et al., 1998). For the calculation of monthly scavenging ratios in Eq. 1, monthly volume-weighted precipitation concentrations and monthly average air concentrations based on ≥15 daily measurements in each month were used. Only daily precipitation concentrations with at least 0.2 mm precipitation amount were included. If there is insufficient data (<15 daily measurements) in each month, the scavenging ratio is not calculated. To account for the dependence on particle size distribution, the scavenging ratio of coarse PM (W_{cPM}) was determined by averaging W_{Ca}, W_{Mg}, and W_{Na} since these base cations are predominantly in coarse PM (Cheng et al., 2015). W_K was used as a surrogate for the scavenging ratio of fine PM (W_{fPM}) for inland sites, whereas $W_{K/2}$ was assumed for coastal sites to take into account the K^+ that may be associated with coarse aerosols (Cheng et al., 2015). Atmospheric K^+ is predominantly associated with fine particles at inland locations, but also associated with coarse sea salt aerosols at coastal locations. In our previous study (Cheng et al., 2015), we observed that the mean W_{fPM} was 34 to 52% of that of W_{cPM} at inland locations, but was 80% at the coastal sites. Therefore, the fine scavenging ratio was reduced by about a factor of 2 at coastal locations. Scavenging ratios and wet scavenging in general are also affected by the chemical composition of aerosols, gas solubilities, temperature, precipitation amount and type, droplet size, nucleation efficiency, vertical concentration differences, and cloud type, which can contribute to the large variability in the scavenging ratios (Cadle et al., 1990; Duce et al., 1991; Galloway et al., 1993).

2.2.4 Relative contributions and scavenging ratios of gaseous and particulate phases

CAPMoN sites measure total NO_3^-, SO_4^{2-}, and NH_4^+ in precipitation. However, wet deposition of NO_3^-, SO_4^{2-}, and NH_4^+ can be attributed to the precipitation scavenging of particulates and gases, such as pNO_3^- and HNO_3, pSO_4^{2-} and SO_2, and pNH_4^+ and NH_3 (Kajino and Aikawa, 2015). To determine their relative contributions and the scavenging ratios of gases, particulate wet scavenging is first determined using W_{cPM}, W_{fPM}, particulate air concentration, and mass fractions in fine and coarse PM. The difference between the total wet scavenging and particulate wet scavenging is assumed to be due to the precipitation scavenging of gases. This assumption was also used in previous studies to estimate NO_3^-, HNO_3, SO_4^{2-}, and SO_2 scavenging ratios (Cadle et al., 1990) and the wet scavenging contributions by gaseous oxidized mercury and particulate mercury (Sakata and Asakura, 2007; Cheng et al., 2015). Eq. 2 was used to determine the wet scavenging of pNO_3^-:

$$[pNO_3^-]_{prec} = W_{fPM}\,[pNO_3^-]_{air}\,P_f + W_{cPM}\,[pNO_3^-]_{air}\,(1-P_f), \quad (2)$$

W_{fPM} and W_{cPM} are the monthly scavenging ratios of fine and coarse PM, respectively (Sect. 2.2.3). $[pNO_3^-]_{air}$ is the monthly average NO_3^- air concentration. P_f is the mass fraction of NO_3^- in fine PM, which varies with air mass origins and tends to form at lower temperatures (Zhang et al., 2008; Zhao and Gao, 2008). A P_f of 0.84 was assumed for the winter months (DJF), whereas 0.29 was used for all other months. These are average mass fractions observed at CAPMoN sites in a short-term field study (Zhang et al., 2008). Eq. 2 accounts for the different scavenging efficiencies of small and large particles.

The contribution of HNO_3 to nitrate wet deposition was calculated using Eq. 3:

$$[HNO_3]_{prec} = [\text{total } NO_3^-]_{prec} - [pNO_3^-]_{prec}, \quad (3)$$

$[\text{total } NO_3^-]_{prec}$ is the monthly volume-weighted NO_3^- precipitation concentration and $[pNO_3^-]_{prec}$ is the wet scavenging of pNO_3^- calculated from Eq. 2. If $[HNO_3]_{prec} < 0$, it is assumed that only pNO_3^- contributed to total nitrate precipitation and no gas scavenging occurred. The relative contributions of particulate and gaseous species to NO_3^- wet deposition were determined using Eq. 4 and 5. Scavenging ratios of pNO_3^- and HNO_3 were determined using Eq. 1.

$$\%pNO_3^- = ([pNO_3^-]_{prec} / [\text{total } NO_3^-]_{prec}) \times 100\%, \quad (4)$$

$$\%HNO_3 = ([HNO_3]_{prec} / [\text{total } NO_3^-]_{prec}) \times 100\%, \quad (5)$$

Similarly, Eq. 2-5 were used to determine the relative contributions of pSO_4^{2-} and SO_2 to total SO_4^{2-} wet deposition and pNH_4^+ and NH_3 to total NH_4^+ wet deposition. A P_f of 0.94 for $[pSO_4^{2-}]_{air}$ and P_f of 0.954 for $[pNH_4^+]_{air}$ was used for all months because these were the average mass fractions observed at CAPMoN sites (Zhang et al., 2008). pSO_4^{2-} and pNH_4^+ have similar P_f because they have similar particle size distributions and often exist together as $(NH_4)_2SO_4$ in the atmosphere. Scavenging ratios for NH_3 were not determined because NH_3 air concentrations were not available.

3 Results and Discussion

3.1 Air concentrations

3.1.1 Geographical patterns

Air concentration statistics and geographical patterns of eight particulate inorganic ions, SO_2, and HNO_3 are plotted in Fig. ~~1a and b~~1. The data were divided into two time periods from 1983-1996 and 1997-2010 to examine potential changes in concentrations due to NO_x and SO_2 emission changes. The range in concentrations (based on the 5th percentile to 95th percentile concentration) from all daily samples at all locations was 0.009-2.9 μg m^{-3} for Ca^{2+}, 0.002-0.5 μg m^{-3} for Mg^{2+}, and 0.006-0.2 μg m^{-3} for K^+ . Larger variability was observed in Ca^{2+} likely because of the variability of soil emissions depending on land use and wind. Large variability is also expected for Na^+ and Cl^- because coastal sites are more frequently impacted by sea-salt aerosols than continental sites. The Na^+ and Cl^- air concentrations ranged from 0.005-1.4 μg m^{-3} and 0.003-1.9 μg m^{-3}, respectively. The range in concentrations were 0.018-5.8 μg m^{-3} for NH_4^+, 0.009-8.7 μg m^{-3} for NO_3^-, and 0.07-14.5 μg m^{-3} for SO_4^{2-}. HNO_3 and SO_2 ranged from 0.014-5.0 μg m^{-3} and 0.011-25.2 μg m^{-3}, respectively. These ions and trace gases are likely to have larger variability in air concentrations than base cations because some sites may be impacted more by anthropogenic emissions, which form secondary pollutants such as SO_4^{2-}, HNO_3, NH_4^+, and NO_3^-, than other sites.

The geographical patterns in air concentrations were examined in greater detail based on the median concentration at each location. Long-term median Ca^{2+} concentrations among the sites ranged from 0.03-0.6 μg m^{-3}. The highest median during both time periods were observed at Longwoods and Egbert, which are the lowest latitude and most inland air concentration sites. Longwoods and Egbert are also predominantly agriculture sites. The median Mg^{2+} concentrations ranged from 0.01-0.09 μg m^{-3}. The highest median was also observed at Longwoods and Egbert. Higher median concentrations were also found at several western Canada sites including at Bratt's Lake, Esther and Saturna in the post-1997 period. The median concentrations ranged from 0.02-0.06 μg m^{-3} for K^+, which is the ion with the least spatial variability in the air concentration. The highest concentrations were observed at Longwoods as well as at Bratt's Lake post-1997. The median Na^+ and Cl^- concentrations ranged from 0.02-0.5 μg m^{-3} and 0.007-0.3 μg m^{-3}, respectively. As expected, the highest median for both ions were observed at the two coastal locations, Saturna and Kejimkujik, due to the proximity to sea-salt aerosol emissions from the ocean. These two sites are the farthest west and east air sampling locations respectively. Na^+ and Cl^- concentrations at Saturna were larger and had greater variability than at Kejimkujik likely because of the higher frequency of marine airflows arriving at Saturna (68% of winds from N and W directions) than at Kejimkujik (31% of winds from E and S directions).

The median NH_4^+ and NO_3^- concentrations ranged from 0.1-1.7 μg m^{-3} and 0.03-2.0 μg m^{-3}, respectively (Fig. 1~~a and b~~). Compared to pre-1997 period, the median concentrations of NH_4^+ and NO_3^- were lower in the post-1997 period. The highest concentrations for both ions were observed at Longwoods and Egbert. Higher concentrations were also found at Sutton, Esther, and at Frelighsburg post-1997. The majority of these sites except for Sutton are agriculture sites located in southern Ontario and Quebec, which implies that higher ammonia emissions from agricultural regions may react with acidic gases in the atmosphere to form particulate ammonium (Pitchford et al. 2009). Acidic gases, such as H_2SO_4 and HNO_3, are produced from the oxidation of SO_2 and NO_x respectively and are primarily emitted from industrial and urban areas. The proximity of these lower latitude air sampling sites to major industrial areas in Ohio and Pennsylvania, USA could result in higher acidic gas concentrations at these sites. This is evident in the air concentration plots for HNO_3 that show higher concentrations of HNO_3 at sites having higher NO_3^-. The median HNO_3 concentrations ranged from 0.07-1.1 μg m^{-3}. Southerly winds also impacted Longwoods, Egbert, and Frelighsburg/Sutton approximately 20%, 32%, and 34% of the time, respectively. The median SO_4^{2-} concentrations among the air sampling sites ranged from 0.6-3.5 μg m^{-3}. The concentrations were lower during the post-1997 than during the pre-1997 period. The highest median concentration was observed at Longwoods. Higher median concentrations were found at several southern Ontario and Quebec sites including Egbert, Sutton, Frelighsburg, Sprucedale, and Chalk River. Larger variability in the concentrations was generally observed across sites in southern and eastern Canada. This pattern is likely attributed to the proximity of the sites to combustion and industrial sources in southern Ontario and Quebec. The southern Canada and Atlantic Canada sites (e.g. Kejimkujik) are downwind of combustion and industrial areas in Ohio and Pennsylvania. In contrast, SO_4^{2-} concentrations at sites located in western and central Canada (e.g., Saturna, Esther, Cree Lake, Bratt's Lake, and ELA) were at or below the overall median concentration of all the sites and had smaller variability.

The median SO_2 concentrations ranged from 0.4-6.4 μg m^{-3} during the 1983-1996 period and from 0.6-2.3 μg m^{-3} post-1997 (Fig. 1b). There was also a reduction in the variability of the concentrations in the post-1997 period. The lower latitude southern Ontario and Quebec sites had higher SO_2 concentrations, whereas western and central Canada sites had much lower concentrations. This geographical pattern is similar to that of SO_4^{2-}. One exception was that the SO_2 concentrations in eastern Canada were similar to or even lower than in western Canada, whereas SO_4^{2-} concentrations in eastern Canada were slightly higher than in western Canada. Eastern Canada sites including Montmorency, Lac Edouard, and Kejimkujik are remote sites; therefore SO_2 concentrations are likely not elevated by the time it arrives at these remote locations since SO_2 can undergo deposition or transform to SO_4^{2-} during transport. The slightly higher SO_4^{2-} in eastern Canada could be from sea-salt sulfate due to the proximity to the Atlantic Ocean.

3.1.2 Temporal patterns

The Kendall slopes and confidence interval in Table 2 shows the annual rate of change in the concentrations of particulate ions and trace gases at the air sampling sites for all years with available data. A significant temporal trend in Ca^{2+} was observed at 5 of 16 sites with no significant changes in the concentrations observed at the remaining sites. Decreasing trends were observed at Saturna, Longwoods, and Egbert, while increasing trends were observed at Esther and Kejimkujik. The largest decline in Ca^{2+} was -16 ng m^{-3} a^{-1} at Longwoods. Overall the temporal changes in Ca^{2+} are small. For Mg^{2+}, a significant decreasing trend was found at Saturna, Longwoods, Chalk River, and Kejimkujik. However, the rate of decline was very small ranging only from -0.5 to -1.1 ng m^{-3} a^{-1}. The rate of decline for K^{+} ranged from -0.5 to -3.8 ng m^{-3} a^{-1} and was observed at 14 of 16 sites. A plot of the annual average K^{+} for ten of the active air sampling sites are shown in Fig. 2a for the 1983-2010 period, which illustrates a gradual decline in K^{+}. Significant decreases in Na^{+} were found at 11 of 16 sites with magnitudes ranging from -0.3 to -4.5 ng m^{-3} a^{-1}. The steepest decline was observed at a coastal site in western Canada. However, increasing trends were observed at two coastal sites in eastern Canada (Montmorency and Kejimkujik). For Cl^{-}, decreasing temporal trends were found at only 6 of 16 sites, suggesting that the temporal trends are not necessarily related to sea-salt emissions. The decline in Cl^{-}, ranging from -0.1 to -0.8 ng m^{-3} a^{-1}, were found at sites in western and central Canada and at Algoma and Longwoods.

NH_4^{+} concentrations have been decreasing at 12 of 16 air sampling sites (Table 2). This result is consistent with the widespread decrease in NH_4^{+} at CAPMoN sites during 1988-2007 (Zbieranowski and Aherne, 2011). The rate of decrease ranged from -4 to -58 ng m^{-3} a^{-1}. The largest declines as shown in Fig. 2b were observed at Longwoods, Egbert, Sprucedale, and Frelighsburg, which are agriculture sites located in southern Ontario and Quebec. The annual decrease was 7.3 times greater than other sites based on the linear regression slopes. The decreasing trend in NH_4^{+} corresponds to the decreasing trend in ammonia emissions in Ontario and Quebec particularly in the post-2002 period (Fig. 2b) (Environment Canada, 2014). Aside from its relationship to ammonia, the negative trend in NH_4^{+} was also strongly tied to trends in NO_3^{-} and SO_4^{2-}. There was an even split in the number of sites with increasing trends and decreasing trends in NO_3^{-}. The rate of increase ranged from 1.3-6.4 ng m^{-3} a^{-1} among active sites, whereas the annual trend was 6-40 ng m^{-3} a^{-1} among inactive sites (e.g. Esther, Sutton, Montmorency). The annual trend in NO_3^{-} decreased from -9.3 to -53 ng m^{-3} a^{-1} at other sites (Table 2). Larger declines were observed at the agriculture sites located in southern Ontario and Quebec. Differences in temporal trends were also observed during different time periods. At 9 of 16 sites, an increasing trend was found between 1991 and 2001 which was followed by a decreasing trend from 2001 to 2010 (Fig. 3). The difference in NO_3^{-} trends between the two decades was also reported in previous analysis of CAPMoN sites (Zbieranowski and Aherne, 2011). The change in NO_3^{-} temporal trends closely resembled that of NO_x emissions in Canada. Between 1991 and 1997, NO_x emissions in Canada increased annually and only began to decrease from 1997 to 2010 (Fig. 3) (Environment Canada, 2014). In the U.S., NO_x emissions were constant over the 1991-1994 period and only began to decrease after 1994 (USEPA, 2015). Reductions in NO_x emissions were implemented following the introduction of the Canada-U.S. Air Quality Agreement and the U.S. Acid

Rain Program and Clean Air Interstate Rule. The decrease in NO_x emissions were largely attributed to lower emissions from stationary fuel combustion and transportation sectors (Lloret and Valiela, 2016).

SO_4^{2-} decreased at a rate of -28 to -109 ng m^{-3} a^{-1} depending on the location (Table 2). The steepest annual declines were observed in the southern Ontario and Quebec region as shown in Fig. 4. The slope of the linear regression equation for the southern Ontario and Quebec sites in Fig. 4 was two times greater than that of other air sampling sites, which are coastal or higher latitude sites distant from major industrial and urban areas. The geographical patterns in the temporal trends of SO_4^{2-} were also similar to those of SO_2 and HNO_3. The annual trends for SO_2 and HNO_3 in the southern Ontario and Quebec region declined 3.8 and 4.9 times faster, respectively, than other air sampling sites across Canada based on the linear regression slopes. Negative trends for SO_4^{2-} and SO_2 concentrations followed the decreasing trend in SO_2 emissions in both Canada and U.S. since 1990 (Environment Canada, 2014; USEPA, 2015) (Fig. 4), corresponding to the period of the Canada-U.S. Air Quality Agreement and the U.S. Acid Rain Program and Clean Air Interstate Rule. Note the steeper decline in SO_2 emissions in Ontario in recent years, which is potentially attributed to the phase-out of coal use in Ontario power plants beginning in 2005 (MOE, 2015).

~~The influence of meteorological parameters including temperature, relative humidity and precipitation rates on the temporal trends of particulate ions and trace gases were also investigated by performing correlation analyses on the monthly averaged data. The descending trend in K^+ between 1993 and 2010 at the majority of the sites was not strongly influenced by precipitation as evident by the weak correlation coefficients (Table S1). Higher correlation between monthly average K^+ and temperature were found at Sprucedale, Frelighsburg and Lac Edouard ($r = 0.52$-0.69, $p<0.05$). At these sites, the monthly average K^+ peaked in March-April and was at the minimum concentration during December-January, which resembled the seasonal temperature cycle (Fig. S2a). The higher K^+ in the early spring could be attributed to increase soil emissions from agriculture operations and forest fires during springtime since the major sources of particulate K^+ are from biomass and soil. Decreasing NH_4^+ observed at most of the sites was only weakly correlated with monthly precipitation rates and relative humidity, implying these meteorological parameters had little influence on the long-term temporal trend. Higher correlation between monthly average NH_4^+ and temperature was found at Kejimkujik ($r = 0.63$, $p<0.05$). The maximum NH_4^+ typically occurred during April-May and reached its lowest concentration during December-January (Fig. S2b). This seasonal trend is linked to the formation of SO_4^{2-} through SO_2 oxidation, which tends to occur at higher temperatures because of increase production of atmospheric oxidants. This theory is consistent with the very high correlation between monthly average NH_4^+ and SO_4^{2-} ($r = 0.91$, $p<0.05$) at Kejimkujik. Overall, strong correlations between NH_4^+ and SO_4^{2-} were observed at all the sites ($r = 0.6$-0.94, $p<0.05$). The high correlation between SO_4^{2-}/SO_2 ratio and temperature ($r = 0.61$-0.84, $p<0.05$) suggests SO_4^{2-} formation from the gas-phase oxidation of SO_2 (Yao et al., 2002). Besides the relationship between NH_4^+ and SO_4^{2-}, three of the sites including Saturna, ELA and Egbert exhibited strong correlations between NH_4^+ and NO_3^- ($r = 0.52$-0.7, $p<0.05$) indicating that NH_4^+ also followed the temporal trend of NO_3^- at some locations. In summary, precipitation and relative humidity had little impact on the long-term temporal patterns of particulate ions. Seasonal~~

~~temperature trends is linked with the seasonal cycle of atmospheric oxidants which explains the short-term patterns in SO_4^{2-} and NH_4^+; however, there is no clear evidence that long-term temperature changes impacted their long-term trends.~~

3.1.3 Aerosol acidity (c/a)

The median c/a ranged from 0.97-1.6 and an overall median c/a of 1.07 was observed across all sites (Fig. 5a). These values are based on inorganic ion contributions to aerosol acidity. Organic acids do not contribute significantly to aerosol acidity compared to the strong inorganic acids (Zhang et al., 2007; Ziemba et al., 2007; He et al., 2012); however, they have been included in the measure of aerosol acidity in some studies (Hennigan et al., 2015 and references therein). Among the sites, the highest aerosol acidity was observed at Kejimkujik because of the higher equivalent anion concentrations relative to cations (Table S2). Higher aerosol acidity was prevalent generally in eastern Canada and central Ontario regions. In contrast to Kejimkujik, the majority of the sites had higher cation than anion concentrations or near equivalent cation and anion concentrations (Table S2). Even though locations like Longwoods and Egbert had greater amount of anions than other locations due to higher NO_3^- and SO_4^{2-}, there were sufficient amounts of cations, mainly NH_4^+, to neutralize the acidic species. While the overall median c/a was close to 1 for all Canadian sites, more than half of the daily c/a data were below 1 at eight locations (Fig. 5a). This suggests there was a substantial amount of time between 1994 and 2010 when aerosols were acidic at some Canadian sites.

A significant increasing trend in the c/a was observed between 1994 and 2010, which indicates a widespread decline in aerosol acidity (Fig. 5b). The rate of decrease in aerosol acidity was small and fairly uniform spatially based on the Kendall slope results. According to Table S2 and Fig. 5b, the annual average cation and anion concentrations and c/a at most of the sites (data combined from 13 of 15 sites) were relatively constant between 1994 and 2000. Since 2001, the annual average cation and anion concentrations and aerosol acidity have been on a slight decline (Table S2). The decrease in cation concentrations appeared consistent with the declining trend in NH_4^+ discussed earlier, since NH_4^+ is the largest contributor to cation concentrations. For anions, NO_3^- and SO_4^{2-} are the predominant ions. Thus, the decline in anions was also consistent with the decreasing rates for NO_3^- and SO_4^{2-}. As mentioned earlier, the decreasing trends in NH_4^+, NO_3^- and SO_4^{2-} were consistent with the reductions in ammonia, NO_x and SO_2 emissions.

3.2 Wet deposition

3.2.1 Geographical patterns

The annual wet deposition statistics for the various ions at the ~~30~~ 31 locations are shown in Fig. 6. The annual wet deposition was based on all years with complete data because the annual flux was determined by summing the daily fluxes. The range in the annual wet deposition based on the 5th and 95th percentile annual wet deposition rate (kg ha^{-1} a^{-1}) was: 0.08-3.6 for Ca^{2+}, 0.02-1.6 for Mg^{2+}, 0.01-0.7 for K^+, 0.03-12.0 for Na^+, 0.06-23.0 for Cl^-, 0.1-6.4 for NH_4^+, 0.4-26.5 for NO_3^-, and 0.5-32.7for SO_4^{2-}. The lowest annual wet deposition rates for Ca^{2+}, Mg^{2+}, Na^+, NH_4^+, NO_3^-, and SO_4^{2-} were observed at

Snare Rapids, which is a remote site in the Northwest Territories of Canada. The highest annual wet deposition recorded at the most eastern coastal site in Bay d'Espoir, Newfoundland were from ions related to sea-salt aerosols, including Na^+, Cl^-, and Mg^{2+}. For Ca^{2+} and ions derived from anthropogenic sources (e.g., NH_4^+, NO_3^-, and SO_4^{2-}), the highest annual wet deposition rates were observed at Priceville and Longwoods, which are the two most southern wet deposition sites in Canada and closest to urban and industrial areas.

Long-term median annual wet deposition of Ca^{2+} ranged from 0.1-2.8 kg ha^{-1} a^{-1} among the wet deposition sites. The highest annual wet deposition was observed at Priceville and Longwoods (Fig. 6). Higher median wet deposition was also found at Algoma, Egbert, and Warsaw Caves. The majority of these sites are agriculture sites. The lowest median wet deposition was observed at the western and eastern coastal sites. The median annual wet deposition of Mg^{2+} ranged from 0.03-1.0 kg ha^{-1} a^{-1}. The highest wet deposition was found at the western and eastern coastal sites with the exception of Goose Bay, which is a higher latitude coastal site located in Labrador. It had the lowest annual precipitation amount among coastal sites in eastern Canada (Fig. S3). Annual Mg^{2+} wet deposition at inland sites was typically at or below the overall median wet deposition for all sites; however, they are slightly higher at Longwoods and Priceville. The median annual wet deposition of K^+ ranged from 0.05-0.4 kg ha^{-1} a^{-1}. Similar to Mg^{2+}, higher annual wet deposition of K^+ was observed at eastern coastal locations with the exception of Goose Bay. Annual wet deposition for inland sites was around the overall median annual wet deposition for all sites except at Longwoods, Algoma and Priceville. The median annual wet deposition of Na^+ and Cl^- ranged from 0.05-7.5 kg ha^{-1} a^{-1} and 0.1-13.6 kg ha^{-1} a^{-1}, respectively. The geographical patterns in the annual wet deposition were similar between Na^+ and Cl^-. Annual wet deposition at western and eastern coastal sites were higher and had greater variability than inland locations.

Median annual NH_4^+ wet deposition ranged from 0.2-5.8 kg ha^{-1} a^{-1} (Fig. 6). Higher annual wet deposition was observed at lower latitude continental sites. Higher latitude continental locations (e.g. Cree Lake, Island Lake, Pickle Lake, Bonner Lake, Chapais) and coastal locations were well below the overall median annual wet deposition. The median annual wet deposition ranged from 0.8-23.3 kg ha^{-1} a^{-1} for NO_3^- and 0.8-26.6 kg ha^{-1} a^{-1} for SO_4^{2-}. These two ions have similar spatial patterns in annual wet deposition. Higher median annual wet deposition occurred at southern Ontario and Quebec sites. Lower median annual wet deposition was observed in eastern Canada. The lowest median annual wet deposition for NO_3^- and SO_4^{2-}, which were well below the overall median annual wet deposition for all sites, was recorded in western and central Canada. These results are consistent with Vet et al. (2014), which observed higher sulfur wet deposition around Lake Ontario and Lake Erie and much lower sulfur wet deposition in western North America than eastern North America.

The geographical patterns in the wet deposition were predominantly affected by the air concentrations. For example, the higher Na^+ and Cl^- wet deposition at coastal locations can be traced back to the higher Na^+ and Cl^- air concentrations. Similarly, the higher NH_4^+, NO_3^- and SO_4^{2-} wet deposition occurring at southern Ontario and Quebec locations was consistent with the geographical patterns in the air concentrations. Although precipitation amount is used to determine wet deposition, only the wet deposition patterns of Mg^{2+} and K^+ were potentially influenced by precipitation amount. As shown in Fig. S3, the annual precipitation amount generally increases from western to eastern sites. Only the Mg^{2+} and K^+ wet deposition were higher at eastern Canada locations.

3.2.2 Temporal trends

Long-term temporal trends in the annual wet deposition of ions were analyzed using Sen's slope (Table 3 and 4) and linear regression analysis. The annual wet deposition of Ca^{2+} and K^+ has not changed significantly at almost all locations. For $Mg^{2+}$and Na^+, there were no significant changes in the annual wet deposition rate at most of the sites, while a very small statistically significant decline in the annual wet deposition was observed at other sites. Of these sites, the rate of decline ranged from -0.001 to -0.008 kg ha^{-1} a^{-1} for Mg^{2+} and -0.002 to -0.02 kg ha^{-1} a^{-1} for Na^+. Decline in base cations has been reported at other Canadian sites during the 1990s (Watmough et al., 2005). The small decrease or lack of change in base cation wet deposition is expected because the major source of base cations at rural Canadian sites are from natural emissions (Watmough et al., 2005). Monitoring the wet deposition Ca^{2+}, Mg^{2+}, K^+, and Na^+ trends are important because these ions neutralize soil acidity and mitigate further harmful impacts to plants and wildlife. A declining trend in the Cl^- wet deposition was observed at 5 of 16 sites (Fig. 7a), and the magnitude ranged from -0.007 to -0.03 kg ha^{-1} a^{-1} (Table 3).

Significant trends in the annual wet deposition of NH_4^+ were observed at only 3 of 16 locations. There were two sites with increasing temporal trend (0.05 kg ha^{-1} a^{-1}), whereas a decreasing trend was found at one location (Table 4). A lack of an overall consistent temporal trend in precipitation NH_4^+ was also found in previous analysis of CAPMoN sites (Zbieranowski and Aherne, 2011). These trends were in contrast to those in the U.S., which has seen an increase in precipitation NH_4^+ at 64% of the wet deposition sites between 1985 and 2004 (Lehmann et al., 2007). While increasing NH_4^+ in precipitation helps to increase precipitation pH and promote plant growth, a counter-effect is that soils can become acidic when NH_4^+ undergoes nitrification (Vogt et al., 2006).

Declining trends in NO_3^- wet deposition was observed at 10 of 16 sites (data combined in Fig. 7a), while no significant trend was found at other locations. The rate of decrease ranged from -0.07 to -1.0 kg ha^{-1} a^{-1} and was largest at the southern Ontario and Quebec sites (Algoma, Longwoods, Egbert, Sprucedale, Frelighsburg, Lac Edouard). One exception was the non-significant trend at Sutton (Table 4) even though this site is only 15 km from Frelighsburg. The discrepancy in the temporal trends at these two sites can be partially attributed to the different measurement periods. Measurements of wet deposition at Sutton ended in 2002, whereas Frelighsburg has been actively measuring wet deposition since 2001. This suggests the rate of decrease in NO_3^- wet deposition was more rapid in the period after 2001 and corresponds with the decline in NO_3^- air concentrations over the same time period discussed earlier. In the U.S. northeast, the decline in precipitation NO_3^- was observed at only 25% of the sites in that region during 1985-2004 (Lehmann et al., 2005). A recent study of NO_3^- wet deposition from 1985-2011 across North America indicates a 40-50% decrease in eastern North America after 2000 (Lloret and Valiela, 2016). Similar to the air concentrations of SO_4^{2-}, decline in SO_4^{2-} wet deposition was also prevalent throughout Canadian sites. This finding is consistent with the decrease in precipitation SO_4^{2-} reported at other Canadian sites during the 1990s (Watmough et al., 2005) and at 89% of the wet deposition sites in the U.S. between 1985 and 2004 (Lehmann et al., 2007). Decreasing temporal trends in SO_4^{2-} wet deposition was found at 11 of 16 sites with magnitudes ranging from -0.1 to -1.0 kg ha^{-1} a^{-1} depending on the location (Table 4). The overall rate of decline was ~2 times higher at the southern Ontario and Quebec sites relative to other locations (Fig. 7b), which is consistent with the patterns in the air concentrations of SO_4^{2-} described earlier. The large declining trends in the wet deposition of nitrogen and sulfur-containing species in conjunction with the relatively smaller declines or lack of change in base cations indicate that acid rain has attenuated over time. This is largely attributed to policies controlling NO_x and SO_2 emissions.

Daily wet deposition of ions was correlated with their respective daily particulate matter concentrations and daily precipitation amount to gain insight into factors influencing the temporal trends in wet deposition. Moderate correlations ($r = 0.38$-0.41, $p<0.05$) between daily wet deposition and particulate matter concentration were found for SO_4^{2-}, Na^+ and Cl^-, whereas only weak correlations were found for other ions. This result partly explains the prevalent decline in wet deposition of SO_4^{2-} and Cl^-. Decreasing NO_3^- wet deposition was also widespread; however it did not strongly correlate with particulate NO_3^- concentrations ($r = 0.21$, $p<0.05$). This is potentially because both gaseous and particulate nitrogen species can contribute to NO_3^- wet deposition. This is supported by the slightly higher correlation ($r = 0.33$, $p<0.05$) between daily NO_3^- wet deposition and HNO_3. For SO_4^{2-} wet deposition which can be attributed to the precipitation scavenging of particulate SO_4^{2-} and SO_2, only a weak correlation was found between daily SO_4^{2-} wet deposition and SO_2 ($r = 0.13$, $p<0.05$). Further analysis on the relative contributions of gaseous and particulate species to NO_3^- and SO_4^{2-} wet deposition will be discussed in Sect. 3.4. Moderate correlations between daily wet deposition and daily precipitation were found for NH_4^+, NO_3^- and SO_4^{2-} ($r = 0.50$-0.56, $p<0.05$), while weaker correlations were found for other ions. Some correlation was expected because wet deposition is determined from precipitation concentration and precipitation amount. On an annual basis, there has been no significant change to the annual precipitation amount at most of the sites, except for significant increases at Bratt's Lake, ELA, Chalk River, and Kejimkujik (Table 4). The lack of change to the annual precipitation is inconsistent with the decreasing trends in SO_4^{2-}, NO_3^- and Cl^- annual wet deposition found at the majority of the sites. Thus, long-term wet deposition of ions was not strongly influenced by long-term precipitation trends between 1983 and 2010.

3.2.3 Acid rain

The geographical patterns in acid rain as measured by precipitation pH are shown in Fig. 8. Precipitation pH is slightly acidic by nature due to the presence of carbonic acid formed by the dissolution of CO_2. A pH below 5 is considered to be acidic precipitation (Lehmann et al., 2007). According to Fig. 8, the median pH in daily precipitation samples across the sites ranged from 4.4-5.7. Between 1983 and 2011, acidic precipitation was observed in more than 50% of the daily precipitation samples at 19 of 31 or 61% of the sites. Acidic precipitation was prevalent in southern Ontario and some parts of eastern Canada, whereas pH was above 5 in western and central Canada. Similarly in regions close to southern Ontario and eastern Canada, higher occurrences of acid rain have been observed in the U.S. northeast region during the 1994-1996 and 2002-2004 periods (Lehmann et al., 2007). Acid rain has contributed to the acidification of soil and lakes (Stoddard et al., 1999; Driscoll et al., 2001; Clair et al., 2002; 2003; Jeffries et al., 2003; Watmough and Dillon, 2003). In the southern Ontario and eastern Canada region, the acid deposition effects are more concerning because the soil is slightly acidic naturally and shallow and the underlying bedrock provides insufficient acid buffering capacity (Clair et al., 2002; Watmough and Dillon, 2003). The geographical patterns in precipitation pH were consistent with those of aerosol acidity discussed earlier. The correlation between the median pH and aerosol acidity (as measured by c/a ratio) among 15 locations was 0.68, which suggests acidic particles partially contributed to acid rain at various Canadian sites.

Between 1983 and 2011, an increasing trend in pH was observed at 13 of 16 sites, while no significant change in pH was found at the remaining three sites (Table 4). The overall decline in acidic precipitation in Canada is consistent with the trends in the U.S. (Lehmann et al., 2007) and H^+ wet deposition trends between 2000-2002 and 2005-2007 periods over most of North America, Europe and Africa (Vet et al., 2014). The rate of increase in pH was slightly higher at southern Ontario and Quebec sites (Table 4). Recent studies indicate there has been a gradual improvement to soil and surface water conditions due to decreases in NO_3^- and SO_4^{2-} wet deposition; however, this recovery has been outpaced by the rate of decline in acidic wet deposition (Strock et al., 2014; Lawrence et al., 2015). The increasing temporal trends in pH can be partially attributed to aerosol acidity. A correlation of 0.29 between daily pH and c/a was found in this study. Based on the annual trend between the 1994 and 2010 period, the annual average pH and c/a (data combined at 13 of 15 sites) had very similar trends (Fig. 5b) and the correlation coefficient improved to 0.86.

3.3 Scavenging ratios

3.3.1 General statistics and comparisons with literature

A summary of the monthly average scavenging ratio (W) (on a mass basis) statistics for the inorganic ions and trace gases are provided in Table S3. Monthly W_{Ca} ranged from 120-14338. The minimum and maximum values were found at Egbert and Algoma, respectively. W_{Mg} ranged from 131-11243. The lowest W was recorded at Chapais, while the highest W was recorded at Kejimkujik. W_{Na} ranged from 76-12165. The lowest W was recorded at Chapais, while the highest W was recorded at Kejimkujik similar to Mg^{2+}. The W_K ranged from 69-5565 and had lower values compared to Ca^{2+}, Mg^{2+}, and Na^+ because K^+ is predominantly in fine particulate matter except for an additional coarse mode found at coastal locations (Zhang et al., 2008). For this reason, it is assumed that the W of fine PM (W_{fPM}) was equivalent to the W_K for inland sites, while $W_{K/2}$ was assumed for coastal sites. The minimum and maximum W_K were found at Montmorency and Kejimkujik, respectively. Since Ca^{2+}, Mg^{2+}, and Na^+ are mainly associated with coarse particulate matter, the average W of these ions was used as an estimate of the W of coarse particles (W_{cPM}). The range of W_{cPM} was 83-12165. The minimum and maximum values were found at Chapais and Kejimkujik, respectively. The W_{Cl} ranged from 210-35521. The minimum and maximum values were found at Chapais and Algoma, respectively. Compared to other ions, W_{Cl} were larger and had greater variability. Overall, the range in the average W for these ions among the 13 sites was within the average W from previous studies (Table S4).

Monthly scavenging ratios were determined for particulate NO_3^- (pNO_3^-) and HNO_3 separately because both gaseous and particulate forms can contribute to NO_3^- wet deposition. Monthly W ranged from 135-4272 for pNO_3^- and 7-16658 for HNO_3. Based on the average scavenging ratio, W_{HNO3} were greater than W_{pNO3}.The average W_{pNO3} from 13 sites were within the range of literature values in Table S4; however the majority of the W_{pNO3} in the literature are determined from total nitrate in precipitation and pNO_3^- in air. Thus, most of the W_{pNO3} are overestimated. Scavenging ratios of pNO_3^- based on total nitrate in precipitation are higher by a factor of 1.4-18 depending on the site (average: factor of 6).

In this study, the average W_{HNO3} at some sites were higher than those in Table S4; however, they were most comparable to the average determined by Cadle et al. (1990) likely because of the similarity in the methods of determining W_{HNO3}. The method first calculates the pNO_3^- scavenged and then the difference between the total NO_3^- and the pNO_3^- scavenged is assumed to be contributed by HNO_3 scavenging. One major difference in the approach was that Cadle et al. (1990) used W_K as a surrogate for W_{pNO3} to estimate the pNO_3^- scavenged, whereas in this study W_{pNO3} considered the seasonal particle size distribution of pNO_3^-. The average W_{HNO3} at some sites in this study were different than those determined by Hicks (2005) (Table S4), who assumed only HNO_3 contributed to NO_3^- wet deposition. The values were also different from that of Kasper-Giebl et al. (1998), who used a multiple linear regression (MLR) approach. For comparison purposes, W_{pNO3} and W_{HNO3} derived from MLR are also shown in Table S4 and S5. The MLR results show $W_{HNO3}>W_{pNO3}$. However, this empirical method generated higher W_{pNO3} and lower W_{HNO3} at some locations compared to the method used in this study. Table S5 indicates that the MLR model fit was considered weak to moderate (R^2= 0.15-0.34) depending on the site.

Monthly W_{pNH4} ranged from 63-4356. The lowest W was recorded at Egbert, while the highest W was recorded at Algoma. Scavenging ratios of NH_3 were undetermined because NH_3 air concentrations were not available. Average W_{pNH4} were also lower than some of the values in the literature (Table S4), which are likely overestimated because the values were based on the total NH_4^+ precipitation concentrations, instead of pNH_4^+ scavenged by precipitation. Comparison of these two methods of calculation indicates that the use of total NH_4^+ precipitation concentration overestimated the scavenging ratios by 4-48% (average: 22%) depending on the location. Despite the coexistence of NH_4^+ and SO_4^{2-} in the atmosphere, the difference between the average scavenging ratios of these ions can vary by 4-98% (average: 32%). The range of monthly scavenging ratios for pSO_4^{2-} and SO_2 were 75-3146 and 0.3-12068, respectively. The average W_{pSO4} among the sites in this study were lower than some of the literature values in Table S4. Most of the studies excluded the wet scavenging of SO_2 because pSO_4^{2-} was assumed to be the dominant contributor to SO_4^{2-} wet deposition. This method overestimates the scavenging ratio of pSO_4^{2-} by 18-85% (average: 44%) compared to the method used in this study. According to the limited number of W_{SO2} estimates (Table S4), the precipitation scavenging of SO_2 is less important compared to pSO_4^{2-} because of the lower W_{SO2}. In this study, SO_2 and pSO_4^{2-} can be equally important at times in terms of scavenging ratios. The average W_{SO2} at more than half of the sites in this study were greater than literature averages. This is potentially due to the different methodologies for calculating W_{SO2} and precipitation type. The MLR method yielded higher W_{pSO4} and lower W_{SO2} at some locations compared to the method used in this study (Table S4 and S5). The approach used in this study was similar to Cadle et al. (1990); however, that study used W_{NH4} as a surrogate for W_{pSO4} based on the assumption these ions are typically found in the same aerosols. There are however large uncertainties with W_{NH4} because of the scavenging by both pNH_4^+ and NH_3. As mentioned earlier, most of the W_{NH4} in literature are overestimated because of the exclusion of NH_3. Use of these values could lead to a high bias in W_{pSO4} and subsequently lower W_{SO2}. Aside from the methodology, the scavenging ratios determined by Cadle et al. (1990) were based on snowfall events, which favor the scavenging of particles over gases (Hicks, 2005; Zhang et al., 2013; 2015).

The variability in scavenging ratios among different ions and trace gases within the same month is shown in Fig. S4. The range in scavenging ratios can be quite large. This is expected because the different physical and chemical properties of the pollutants affect their wet scavenging efficiencies. For particulate matter, coarse particles (e.g., Ca^{2+}, Mg^{2+} and Na^+) are scavenged more efficiently than fine particles (e.g. K^+) (Galloway et al., 1993; Guerzoni et al., 1995; Tuncel and Ungör, 1996). The different solubilities of gaseous pollutants (HNO_3 and SO_2) can also explain the differences in scavenging ratios for different pollutants. W_{HNO3} were 1.4 to 6 times higher than those of W_{SO2} depending on the location (Table S3), which is consistent with the higher solubility of HNO_3 compared to SO_2 (H = 2.1 x 10^5 M atm^{-1} vs. 1.2 M atm^{-1}; Zhang et al., 2006; Sander, 2015).

3.3.2 Variations in scavenging ratios

Although the monthly scavenging ratios of most ions span a wide range, the average scavenging ratios of particulate ions were within a factor of 1.6-4.5 among the 13 sites (Table S3). The average scavenging ratios of Na^+, Cl^- and Ca^{2+} have larger spatial variability than other particulate ions. This may reflect the different precipitation scavenging efficiencies of particles in the marine boundary layer and continental atmospheres as hypothesized by Galloway et al. (1993). One related theory is that the higher relative humidity in marine environments is conducive to the hygroscopic growth of sea-salt aerosols which increases its scavenging efficiency (Hennigan et al., 2008). The average scavenging ratios ranged from 497-996 for fine particles (factor of 2 spatial variability) and 666-2077 for coarse particles (factor of 3 spatial variability). Larger scavenging ratios of fine particles were found at inland sites, where soil and biomass emissions are sources of K^+. For coarse particles, the larger scavenging ratios at coastal sites (Table S3) were likely attributed to oceanic source of Na^+ and Mg^{2+}. The greatest spatial variability was in the scavenging ratios of gases including HNO_3 and SO_2. The average scavenging ratios varied by a factor 7.4 and 10.7, respectively. The large variability in scavenging ratios between sites is expected because the air and precipitation concentrations and precipitation type and amounts among other factors can also vary with location.

A pronounced seasonal variation can be seen in the monthly average scavenging ratios. The average scavenging ratio of most of the ions and HNO_3 were lowest during July or August (Fig. S5), which resembles the monthly NO_3^-, SO_4^{2-}, and NH_4^+ variations in a previous study (Kasper-Giebl et al., 1998). There were two periods when the average scavenging ratios peaked: one peak during April-May and a second peak during September-October were observed for most of the ions and HNO_3. A similar pattern was obtained for W_{pNO3} when MLR was used to generate monthly scavenging ratios. However, different patterns were obtained for W_{HNO3} and W_{pSO4} derived from MLR, as shown by the higher values during winter and lower values in the warm seasons (Fig. S5 and Table S6).

Monthly variations in W_{SO2} were different from those of other ions and HNO_3. The average W_{SO2} were lower during winter and peaked in the summer, and is supported by the MLR results as well (Fig. S5 and Table S6). This result is also consistent with the seasonal W_{SO2} patterns from multiple U.S. sites (Hicks, 2005) and other studies suggesting the inefficient scavenging of SO_2 by snow (Kasper-Giebl et al., 1998 and references therein). However, limited field measurements of dissolved SO_2 (measured as sulfite) in precipitation samples indicate that the highest precipitation concentrations were found in the colder months, which is consistent with solubility theory (Hales and Dana, 1979; Dana, 1980). This finding does not necessarily contradict the results from this study because W_{SO2} also depend on the air concentration. The higher ambient SO_2 likely due to higher combustion emissions associated with winter heating (Fig. S6) resulted in lower scavenging ratios, and vice-versa during warmer months. Besides temperature effects on solubility, precipitation pH and the presence of NH_3 and H_2O_2 could also affect SO_2 wet scavenging (Zhang et al., 2006).

Most of the long-term scavenging ratio trends were not statistically significant according to the Seasonal Kendall test, but some statistically significant trends were found at a few locations and for some nitrogen and sulfur species. At Longwoods, there was a statistically significant declining trend in the scavenging ratio of pNO_3^-; however the magnitude of the trend was only -6.3 (<1%) per year which is small compared to the scavenging ratio (values in the hundreds to thousands). At Algoma, a significant increasing trend in the scavenging ratio of pSO_4^{2-} was found with a slope of +11.4 (1.4%) per year. At many of the sites, the lack of long-term trends in the scavenging ratios of sulfur and nitrogen species reflect the decreasing trends in both wet deposition and air concentrations (Table 2 and 4). There are also many factors that can affect the precipitation concentrations, such as particle sizes, air concentrations, rainfall intensity, and precipitation and cloud types, which vary geographically and could change over time.

3.4 Relative contributions of particulates and gases to nitrate, ammonium and sulfate wet deposition

In the previous section, scavenging ratios were determined for particulate (pNO_3^-, pNH_4^+, pSO_4^{2-}) and gaseous (HNO_3 and SO_2) species. In this section, the relative percent contributions of these particulate and gaseous species to nitrate, ammonium, and sulfate wet deposition are determined. The average $\pm$ 1σ of pNO_3^- contributions to nitrate wet scavenging (%pNO_3^-) was 28±23% for all years of data at the 13 locations. Percent HNO_3 contributions to nitrate wet scavenging (%HNO_3) was 72±23%. Based on the average, %HNO_3 dominated %pNO_3^- at most of the sites (Fig. 9a). Geographical variations were observed in the %pNO_3^- and %HNO_3. Average %pNO_3^- were higher at the two lowest latitude sites and coastal sites (Fig. 9a). One reason is because of the higher pNO_3^- air concentrations at the lower latitude locations (Longwoods and Egbert) discussed in Sect. 3.1.1. %pNO_3^- were also higher at the coastal locations (Saturna and Kejimkujik) likely because of the partitioning of HNO_3 to sea-salt aerosols (Pryor and Sørensen, 2000; Fischer et al., 2006), which are typically coarse particles and hygroscopic and hence more efficiently removed by precipitation. In contrast, %HNO_3 were greater at the higher latitude continental locations (Fig. 9a). Relative contributions of pNH_4^+ and NH_3 were 70±19% and 30±19%, respectively. Precipitation scavenging of pNH_4^+ was greater than NH_3 at all sites (Fig. 9b). The percent pSO_4^{2-} contributions to sulfate wet scavenging (%pSO_4^{2-}) was 63±20%, while percent SO_2 contributions to sulfate wet scavenging (%SO_2) was 37±20%. Average %pSO_4^{2-} were greater than that of %SO_2 at most of the sites (Fig. 9c). No pronounced geographical patterns were observed in the relative contributions of gases and particulates to ammonium or sulfate wet deposition. Knowledge of the relative scavenging contributions of gases and particles may improve the wet deposition modeling of nitrate, ammonium, and sulfate, which continues to show discrepancies between model and observations (Appel et al., 2011; Zhang et al., 2012; Kajino and Aikawa, 2015; Qiao et al., 2015). Furthermore, gas- and particulate-phase pollutants may not come from the same source, since particulate matter can be re-emitted from natural sources and human activity. Aerosol formation is modeled separately in chemical transport models and the wet deposition of particles and gases use different parameterizations in these models. The scavenging coefficient of gases in models depends on Henry's law constant or gas diffusivity and reactivity, whereas the scavenging coefficient of particles is a function of particle size distribution and collection efficiency among other factors (Gong et al., 2011). Studies also suggest different efficiencies between rainout and washout scavenging mechanisms for gases and aerosols (Gong et al., 2011; Kajino and Aikawa, 2015). These parameterizations can differ between different chemical transport models as well leading to large uncertainties in the wet deposition estimates (Tost et al., 2007). Gas/aerosol wet scavenging observations can also be used to evaluate those from wet deposition simulations (Kajino and Aikawa, 2015).

A seasonal variation was observed in the relative contributions of gases and particulates to nitrate, ammonium, and sulfate wet deposition. The contributions by particulates to nitrate, ammonium, and sulfate wet scavenging were greater during cold months and lower during summer (Fig. 10). This pattern is consistent with studies suggesting that particle scavenging by snow is more efficient than the scavenging by rain for an equivalent amount of precipitation (Zhang et al., 2013, 2015). Based on scavenging ratios, Zhang et al. (2015) found that snow scavenging can be 10 times more efficient than the rain scavenging of polycyclic aromatic compounds (PAC), and that snow scavenging of particulate-phase PAC can exceed that of gas-phase PAC by a similar magnitude. In contrast to particle scavenging, greater precipitation scavenging of gases was observed in the warm seasons (Fig. 10). This inverse relationship between particle and gas wet scavenging resulted because of Eq. 3, which assumes that the precipitation scavenging in excess of particle wet scavenging was due to gas scavenging. This assumption needs to be validated by independently deriving the gas scavenging contributions; however, the results based on the assumption are consistent with precipitation scavenging theories.

In terms of nitrate scavenging, the largest difference between gas and particulate wet scavenging were observed during warm months (factor of 4 higher for HNO_3), whereas smaller differences were seen during cold months (Fig. 10a). The large contribution by HNO_3 is expected because it is one of the most soluble gases and is effectively scavenged by rainout (Chang, 1984; Garrett et al., 2006). %HNO_3 were also fairly high during the cold months because of higher solubility at lower temperatures and the high absorption and retention of HNO_3 and other strong acids on ice crystals (Diehl et al., 1995; Clegg and Abbatt, 2001). Snow scavenging of HNO_3 can also exceed below-cloud rain scavenging of HNO_3 for an equivalent precipitation rate (Chang, 1984).

Particle wet scavenging exceeded gas scavenging contributions to ammonium wet deposition in most months by a factor of 2.6 except during May-June (Fig. 10b). For sulfate scavenging, larger differences between gas and particulate wet scavenging were found during cold months (factor of 2 higher for pSO_4^-), while small differences were observed during warm months (Fig. 10c). The greater scavenging of pSO_4^- during colder months is likely attributed to the effectiveness of particle scavenging by snow as discussed earlier. Another explanation for the large disparity between particle and gas scavenging in the cold months could be the low absorption of SO_2 by ice crystals especially on low pH ice surfaces (Clegg and Abbatt, 2001). As for the smaller difference between particle and gas scavenging during warm months, experiments suggest that snow scavenging of SO_2 can be increased by the presence of H_2O_2 and relatively higher temperatures of ~0^oC (Mitra et al., 1990). The latter conditions are conducive to the formation of a quasi-liquid layer on the ice surface, which may increase the dissolution of SO_2 (Clegg and Abbatt, 2001).

4 Conclusions

Long-term air concentrations, wet deposition, and scavenging ratios of inorganic ions were analyzed using CAPMoN data. Geographical variability in the air concentrations of inorganic ions can be attributed to proximity of the sites to anthropogenic sources, oceanic sea-salt emissions, and agricultural emissions. Annual wet deposition geographical patterns for Ca^{2+}, Na^+, Cl^-, NH_4^+, NO_3^-, and SO_4^{2-} were similar to those in air. Widespread declines were observed for NH_4^+ (1994-2010) and SO_4^{2-} (1983-2010) in air, which was attributed to decreases in SO_2, NO_x, and local NH_3 emissions. NO_3^- air concentrations increased from 1991-2001 and then decreased from 2001-2010, consistent with the trends in NO_x emissions in Canada over these two decades and in the U.S. over the last decade. However, widespread declines in annual wet deposition were only found for NO_3^- and SO_4^{2-} from 1984-2011. SO_4^{2-} air concentrations and annual wet deposition declined ~2 times faster in southern Ontario and southern Quebec than other locations because of the proximity of the sites to industrial emission sources. Aerosol acidity and acid rain had greater impacts to southern and eastern Canada than western Canada. Temporal trends show aerosol acidity and acid rain have been decreasing simultaneously from 1994-2010, consistent with large declines in nitrate and sulfur species and slight declines or lack of change in base cations.

Scavenging ratios of particulate NH_4^+, SO_4^{2-} and NO_3^- in literature may be overestimated on average by 22%, 44% and a factor of 6, respectively, because the wet scavenging of gases were excluded. The wet scavenging of HNO_3 dominated particulate NO_3^- at most locations, while the wet scavenging of particulate NH_4^+ and SO_4^{2-} were more efficient than NH_3 and SO_2, respectively. The wet scavenging of particles was more efficient in the cold months likely because of the scavenging by snow. Greater gas scavenging was found in the warm months opposite in trend to particulate wet scavenging.

Long-term trends in inorganic ions provide greater insight into which Canadian regions are still susceptible to or likely recovering from acid rain impacts, and the effectiveness of environmental policies at mitigating acid rain. Particulate inorganic ions and trace gas scavenging ratios provide a measure of the wet scavenging efficiencies and are potentially useful surrogates for the wet scavenging of other pollutants provided that they have similar physicochemical properties (e.g. solubility, particle sizes, etc.). These results can be considered in future wet deposition modeling to improve the prediction of nitrate, ammonium, and sulfate wet deposition. Scavenging ratios can potentially be used to obtain a rough first order estimate of the wet deposition at other locations considering the uncertainties in both the scavenging ratios and in wet deposition modeling.

Data availability

The datasets used in this study can be accessed from the websites in the reference list or by contacting the corresponding author.

Competing interests

The authors declare that they have no conflict of interest.

Acknowledgements

The authors gratefully acknowledge the CAPMoN team of Environment and Climate Change Canada (ECCC) and the Canadian National Atmospheric Chemistry (NAtChem) Particulate Matter and Precipitation Databases and its data contributing agencies/organizations for the provision of data (1983-2011) used in this publication. The authors thank Chantale Cerny, Samantha Lee, and Bill Sukloff from ECCC for advice on climate data extraction.

References

Appel, K. W., Foley, K. M., Bash, J. O., Pinder, R. W., Dennis, R. L., Allen D. J., and Pickering, K.: A multi-resolution assessment of the Community Multiscale Air Quality (CMAQ) model v4.7 wet deposition estimates for 2002–2006, Geosci. Model Dev., 4, 357-371, doi:10.5194/gmd-4-357-2011, 2011.

Bourcier, L., Masson, O., Laj, P., Chausse, P., Pichon, J. M., Paulat, P., Bertrand, G., and Sellegri, K.: A new method for assessing the aerosol to rain chemical composition relationships, Atmos. Res., 118, 295-303, 2012.

Cadle, S. H., VandeKopple, R., Mulawa, P. A., and Dasch, J. M.: Ambient concentrations, scavenging ratios, and source regions of acid related compounds and trace metals during winter in northern Michigan, Atmos. Environ., 24(12), 2981-2989, 1990.

Chang, T. Y.: Rain and snow scavenging of HNO3 vapor in the atmosphere, Atmos. Environ. (1967), 18(1), 191-197, 1984.

Cheng, I., Zhang, L., and Mao H.: Relative contributions of gaseous oxidized mercury and fine and coarse particle-bound mercury to mercury wet deposition at nine monitoring sites in North America, J. Geophys. Res. Atmospheres, 120(16), 8549-8562, 2015.

Clair, T. A., Ehrman, J. M., Ouellet, A. J., Brun, G., Lockerbie, D., and Ro, C. -U. : Changes in freshwater acidification trends in Canada's Atlantic provinces: 1983–1997, Water Air Soil Pollut., 135(1-4), 335-354, 2002.

Clegg, M., and Abbatt, D.: Uptake of gas-phase SO2 and H2O2 by ice surfaces: dependence on partial pressure, temperature, and surface acidity, J. Phys. Chem. A, 105(27), 6630-6636, 2001.

Cole, A. S., Steffen, A., Eckley, C. S., Narayan, J., Pilote, M., Tordon, R., Graydon, J. A., St. Louis, V. L., Xu, X., and Branfireun, B. A.: A survey of mercury in air and precipitation across Canada: patterns and trends, Atmosphere, 5(3), 635-668, 2014.

Dana, M. T.: SO2 versus sulfate wet deposition in the eastern United States, J. Geophys. Res. Oceans, 85(C8), 4475-4480, 1980.

Diehl, K., Mitra, S. K., and Pruppacher, H. R.: A laboratory study of the uptake of HNO3 and HCl vapor by snow crystals and ice spheres at temperatures between 0 and − 40 C, Atmos. Environ., 29(9), 975-981, 1995.

Driscoll, C. T., Lawrence, G. B., Bulger, A. J., Butler, T. J., Cronan, C. S., Eagar, C., Lambert, K. F., Likens, G. E., Stoddard, J. L., and Weathers, K. C.: Acidic Deposition in the Northeastern United States: Sources and Inputs, Ecosystem Effects, and Management Strategies, Bioscience, 51(3), 180-198, 2001.

Driscoll, C. T., Driscoll, K. M., Roy, K. M., and Mitchell, M. J.: Chemical response of lakes in the Adirondack region of New York to declines in acidic deposition, Environ. Sci. Technol., 37(10), 2036-2042, 2003.

Duce, R. A., Liss, P. S., Merrill, J. T., Atlas, E. L., Buat-Menard, P., Hicks, B. B., Miller, J.M., Prospero, J. M., Arimoto, R., Church, J. M., Ellis, W., Galloway, J. N., Hansen, L., Jickells, T. D., Knap, A. H., Reinhardt, K. H., Schneider, B., Soudine, A., Tokos, J. J., Tsunogai, S., Wollast, R., and Zhou, M.: The atmospheric input of trace species to the world ocean, Global Biogeochem. Cycles, 5, 193-259, 1991.

Encinas, D., Calzada, I., and Casado, H.: Scavenging ratios in an urban area in the Spanish Basque country, Aerosol Sci. Technol., 38(7), 685-691, 2004.

Environment Canada: National Pollutant Release Inventory (NPRI), Air pollutant emission inventory – online data search, Emission trends, available at: http://www.ec.gc.ca/inrp-npri/donnees-data/ap/index.cfm?lang=En, 2014 (Accessed 15 December 2015)

Environment Canada: Canadian National Atmospheric Chemistry (NAtChem) Particulate Matter and Precipitation Chemistry Database. Science and Technology Branch, 4905 Dufferin Street, Toronto, Ontario, Canada M3H 5T4. Available at: http://www.on.ec.gc.ca/natchem/Login/Login.aspx, 2015a (Accessed 1 October 2015)

Environment Canada: Canadian Climate Data Archives, Ontario Climate Center, Meteorological Service of Canada, 4905 Dufferin Street, Toronto, Ontario, Canada M3H 5T4, 2015b.

Fischer, E., Pszenny, A., Keene, W., Maben, J., Smith, A., Stohl, A., and Talbot, R.: Nitric acid phase partitioning and cycling in the New England coastal atmosphere, J. Geophys. Res. Atmospheres, 111, D23S09, doi:10.1029/2006JD007328, 2006.

Galloway, J. N., Savoie, D. L., Keene, W. C., and Prospero, J. M.: The temporal and spatial variability of scavenging ratios for NSS sulfate, nitrate, methanesulfonate and sodium in the atmosphere over the North Atlantic Ocean, Atmos. Environ., 27(2), 235-250, 1993.

Garrett, T. J., Avey, L., Palmer, P. I., Stohl, A., J. Neuman, A., Brock, C. A., Ryerson, T. B., Holloway, J. S.: Quantifying wet scavenging processes in aircraft observations of nitric acid and cloud condensation nuclei, J. Geophys. Res. Atmospheres, 111, D23S51, doi:10.1029/2006JD007416, 2006.

Gilbert, R. O.: Statistical Methods for Environmental Pollution Monitoring, Van Nostrand Reinhold Company Inc., New York, USA, 1987.

Gong, W., Stroud, C., and Zhang, L.: Cloud processing of gases and aerosols in air quality modeling, Atmosphere, 2(4), 567-616, 2011.

Granat, L., Engström, J. E., Praveen, S., and Rodhe, H.: Light absorbing material (soot) in rainwater and in aerosol particles in the Maldives, J. Geophys. Res. Atmospheres, 115(D16307), doi:10.1029/2009JD013768, 2010.

Guerzoni, S., Cristini, A., Caboi, R., Le Bolloch, O., Marras, I., and Rundeddu, L.: Ionic composition of rainwater and atmospheric aerosols in Sardinia, southern Mediterranean, Water Air Soil Pollut., 85(4), 2077-2082, 1995.

Hales, J. M. and Dana, M. T.: Regional-scale deposition of sulfur dioxide by precipitation scavenging, Atmos. Environ., 13(8), 1121-1132, 1979.

Hames, R. S., Rosenberg, K. V., Lowe, J. D., Barker, S. E., and Dhondt, A. A.: Adverse effects of acid rain on the distribution of the Wood Thrush Hylocichla mustelina in North America, Proc. Natl. Acad. Sci., 99(17), 11235-11240, 2002.

He, J., and Balasubramanian, R.: Rain-aerosol coupling in the tropical atmosphere of Southeast Asia: distribution and scavenging ratios of major ionic species, J. Atmos. Chem., 60(3), 205-220, 2008.

He, K., Zhao, Q., Ma, Y., Duan, F., Yang, F., Shi, Z., and Chen, G.: Spatial and seasonal variability of PM 2.5 acidity at two Chinese megacities: insights into the formation of secondary inorganic aerosols, Atmos. Chem. Phys., 12(3), 1377-1395, 2012.

Hedin, L. O., Granat, L., Likens, G. E., Adri Buishand, T., Galloway, J. N., Butler, T. J., and Rodhe, H.: Steep declines in atmospheric base cations in regions of Europe and North America, Nature, 367, 351-354, 1994.

Hennigan, C. J., Bergin, M. H., Dibb, J. E., and Weber, R. J.: Enhanced secondary organic aerosol formation due to water uptake by fine particles, Geophys. Res. Lett., 35(18), L18801, doi:10.1029/2008GL035046, 2008.

Hennigan, C. J., Izumi, J., Sullivan, A. P., Weber, R. J., and Nenes, A.: A critical evaluation of proxy methods used to estimate the acidity of atmospheric particles, Atmos. Chem. Phys., 15(5), 2775-2790, 2015.

Hicks, B. B.: A climatology of wet deposition scavenging ratios for the United States, Atmos. Environ., 39(9), 1585-1596, 2005.

Jeffries, D. S., Brydges, T. G., Dillon, P. J., and Keller, W.: Monitoring the results of Canada/USA acid rain control programs: some lake responses, Environ. Monit. Assess., 88(1-3), 3-19, 2003.

Kajino, M. and Aikawa, M.: A model validation study of the washout/rainout contribution of sulfate and nitrate in wet deposition compared with precipitation chemistry data in Japan, Atmos. Environ., 117, 124-134, 2015.

Kasper-Giebl, A., Kalina, M. F., and Puxbaum, H.: Scavenging ratios for sulfate, ammonium and nitrate determined at Mt. Sonnblick (3106 m.a.s.l.), Atmos. Environ., 33(6), 895-906, 1999.

Kerminen, V. M., Hillamo, R., Teinilä, K., Pakkanen, T., Allegrini, I., and Sparapani, R.: Ion balances of size-resolved tropospheric aerosol samples: implications for the acidity and atmospheric processing of aerosols, Atmos. Environ., 35(31), 5255-5265, 2001.

Kothawala, D. N., Watmough, S. A., Futter, M. N., Zhang, L., and Dillon, P. J.: Stream nitrate responds rapidly to decreasing nitrate deposition. Ecosystems, 14, 274-286, 2011.

Kulshrestha, U. C., Reddy, L. A. K., Satyanarayana, J., and Kulshrestha, M. J.: Real-time wet scavenging of major chemical constituents of aerosols and role of rain intensity in Indian region, Atmos. Environ., 43(32), 5123-5127, 2009.

Lawrence, G. B., Hazlett, P. W., Fernandez, I. J., Ouimet, R., Bailey, S. W., Shortle, W. C., Smith, K. T., and Antidormi, M. R.: Declining Acidic Deposition Begins Reversal of Forest-Soil Acidification in the Northeastern US and Eastern Canada, Environ. Sci. Technol., 49(22), 13103-13111, 2015.

Lehmann, C. M., Bowersox, V. C., and Larson S. M.: Spatial and temporal trends of precipitation chemistry in the United States, 1985–2002, Environ. Pollut., 135(3), 347-361, 2005.

Lehmann, C. M., Bowersox, V. C., Larson, R. S., and Larson, S. M.: Monitoring long-term trends in sulfate and ammonium in US precipitation: Results from the National Atmospheric Deposition Program/National Trends Network, Water Air Soil Pollut., 7, 59-66, 2007.

Lloret, J. and Valiela, I.: Unprecedented decrease in deposition of nitrogen oxides over North America: the relative effects of emission controls and prevailing air-mass trajectories, Biogeochem., doi:10.1007/s10533-016-0225-5, 2016.

McMillan, A. C., MacIver, D., and Sukloff, W. B.: Atmospheric environmental information—an overview with Canadian examples, Environ. Modell. Softw., 15(3), 245-248, 2000.

Mitra, S. K., Barth, S. and Pruppacher, H. R.: A laboratory study on the scavenging of SO2 by snow crystals, Atmos. Environ., 24(9), 2307-2312, 1990.

Ontario Ministry of Energy (MOE): The End of Coal, available at: http://www.energy.gov.on.ca/en/archive/the-end-of-coal/, 2015 (Accessed 3 February 2016)

Pitchford, M. L., Poirot, R. L., Schichtel, B. A., and Maim, W. C.: Characterization of the winter midwestern particulate nitrate bulge, J. Air Waste Manag. Assoc., 58(9), 1061–9, 2009.

Prestbo, E. M. and Gay, D. A.: Wet deposition of mercury in the US and Canada, 1996–2005: Results and analysis of the NADP mercury deposition network (MDN), Atmos. Environ., 43(27), 4223-4233, 2009.

Pryor, S. C. and Sørensen, L. L.: Nitric acid-sea salt reactions: Implications for nitrogen deposition to water surfaces, J. Appl. Meteorol., 39(5), 725-731, 2000.

Qiao, X., Tang, Y., Hu, J., Zhang, S., Li, J., Kota, S. H., Wu, L., Gao, H., Zhang, H., and Ying, Q.: Modeling dry and wet deposition of sulfate, nitrate, and ammonium ions in Jiuzhaigou National Nature Reserve, China using a source-oriented CMAQ model: Part I. Base case model results, Sci. Total Environ., 532, 831-839, 2015.

Sakata, M., and Asakura, K.: Estimating contribution of precipitation scavenging of atmospheric particulate mercury to mercury wet deposition in Japan, Atmos. Environ., 41(8), 1669-1680, 2007.

Sander, R.: Compilation of Henry's law constants (version 4.0) for water as solvent, Atmos. Chem. Phys., 15(8), 4399-4981, 2015.

Shrestha, A. B., Wake, C. P., Dibb, J. E., and Whitlow, S. I.: Aerosol and precipitation chemistry at a remote Himalayan site in Nepal, Aerosol Sci. Technol., 36(4), 441-456, 2002.

Stoddard, J. L., Jeffries, D. S., Lükewille, A., Clair, T. A., Dillon, P. J., Driscoll, C. T., Forsius, M., Johannessen, M., Kahl, J. S., Kellogg, J. H., and Kemp, A.: Regional trends in aquatic recovery from acidification in North America and Europe, Nature, 401(6753), 575-578, 1999.

Strock, K. E., Nelson, S. J., Kahl, J. S., Saros, J. E., and McDowell, W. H.: Decadal trends reveal recent acceleration in the rate of recovery from acidification in the northeastern US, Environ. Sci. Technol., 48(9), 4681-4689, 2014.

Tost, H., Jöckel, P., Kerkweg, A., Pozzer, A., Sander, R., and Lelieveld J.: Global cloud and precipitation chemistry and wet deposition: tropospheric model simulations with ECHAM5/MESSy1, Atmos. Chem. Phys., 7(10), 2733-2757, 2007.

Tuncel, S. G. and Ungör, S.: Rain water chemistry in Ankara, Turkey, Atmos. Environ., 30(15), 2721-2727, 1996.

USEPA: 2011 National Emissions Inventory Data, available at: http://www3.epa.gov/ttnchie1/net/2011inventory.html, 2015 (Accessed 15 December 2015)

Vet, R., Artz, R.S., Carou, S., Shaw, M., Ro, C.U., Aas, W., Baker, A., Bowersox, V.C., Dentener, F., Galy-Lacaux, C. and Hou, A., Pienaar, J. J., Gillett, R., Forti, M. C., Gromov, S., Hara, H., Khodzher, T., Mahowald, N. M., Nickovic, S., Rao, P.

S. P., and Reid, N. W.: A global assessment of precipitation chemistry and deposition of sulfur, nitrogen, sea salt, base cations, organic acids, acidity and pH, and phosphorus, Atmos. Environ., 93, 3-100, 2014.

Vogt, R. D., Seip, H. M., Larssen, T., Zhao, D., Xiang, R., Xiao, J., Luo, J., and Zhao, Y.: Potential acidifying capacity of deposition: Experiences from regions with high NH4+ and dry deposition in China, Sci. Total Environ., 367(1), 394-404, 2006.

Wang, X., Zhang, L., and Moran, M. D.: Bulk or modal parameterizations for below-cloud scavenging of fine, coarse, and giant particles by both rain and snow, J. Adv. Model Earth Sy., 6(4), 1301-1310, 2014.

Watmough, S. A. and Dillon, P. J.: Base cation and nitrogen budgets for a mixed hardwood catchment in south-central Ontario, Ecosystems, 6(7), 675-693, 2003.

Watmough, S. A., Aherne, J., Alewell, C., Arp, P., Bailey, S., Clair, T., Dillon, P., Duchesne, L., Eimers, C., Fernandez, I., and Foster, N.: Sulphate, nitrogen and base cation budgets at 21 forested catchments in Canada, the United States and Europe, Environ. Monit. Assess., 109(1-3), 1-36, 2005.

Yao, X., Chan, C. K., Fang, M., Cadle, S., Chan, T., Mulawa, P., He, K., and Ye, B.: The water-soluble ionic composition of PM2.5 in Shanghai and Beijing, China, Atmos. Environ., 36(26), 4223-4234, 2002.

Zbieranowski, A. L. and Aherne, J.: Long-term trends in atmospheric reactive nitrogen across Canada: 1988–2007, Atmos. Environ., 45(32), 5853-5862, 2011.

Zhang, L., Vet, R. and Michelangeli, D. V.: Numerical investigation of gas scavenging by weak precipitation, J. Atmos. Chem., 54(3), 203-231, 2006.

Zhang, L., Jacob, D. J., Knipping, E. M., Kumar, N., Munger, J. W., Carouge, C. C., van Donkelaar, A., Wang, Y. X., and Chen, D.: Nitrogen deposition to the United States: distribution, sources, and processes, Atmos. Chem. Phys., 12, 4539-4554, doi:10.5194/acp-12-4539-2012, 2012.

Zhang, L., Vet, R., Wiebe, A., Mihele, C., Sukloff, B., Chan, E., Moran, M. D., and Iqbal, S.: Characterization of the size segregated water-soluble inorganic ions at eight Canadian rural sites. Atmos. Chem. Phys., 8, 7133–7151, doi:10.5194/acp-8-7133-2008, 2008.

Zhang, L., Wang, X., Moran, M. D., and Feng, J.: Review and uncertainty assessment of size-resolved scavenging coefficient formulations for below-cloud snow scavenging of atmospheric aerosols, Atmos. Chem. Phys., 13, 10005–10025, doi:10.5194/acp-13-10005-2013, 2013.

Zhang, L., Cheng, I., Muir, D., and Charland, J. -P.: Scavenging ratios of polycyclic aromatic compounds in rain and snow at the Athabasca oil sands region, Atmos. Chem. Phys., 15, 1421–1434, 2015.

Zhang, Q., Jimenez, J. L., Worsnop, D. R., and Canagaratna, M.: A case study of urban particle acidity and its influence on secondary organic aerosol, Environ. Sci. Technol., 41(9), 3213-3219, 2007.

Zhao, Y. and Gao, Y.: Mass size distributions of water-soluble inorganic and organic ions in size-segregated aerosols over metropolitan Newark in the US east coast, Atmos. Environ., 42(18), 4063-4078, 2008.

Ziemba, L. D., Fischer, E., Griffin, R. J., and Talbot, R. W.: Aerosol acidity in rural New England: Temporal trends and source region analysis, J. Geophys. Res. Atmos., 112(D10S22), doi:10.1029/2006JD007605, 2007.

Table 1: Site and data descriptions. NA indicates no available data. Short-term data were not analyzed. Refer to Fig. S1 for a map of the sites.

Site name	Province	Latitude	Longitude	Elevation (m)	Coastal/inland	Land use	Air data	Wet deposition data
Saturna	BC	48.78	-123.13	178	Coastal	Forest	Dec 1990-Dec 2010	Jan 1990-Dec 2011
Snare Rapids	NT	63.52	-116.00	240	Inland	Forest	NA	Jan 1989-Dec 2011
Esther	AB	51.67	-110.20	707	Inland	Agricultural	Oct 1991-Mar 2003	Jan 1987-Dec 2002, Jan 2009-Dec 2011
Cree Lake	SK	57.35	-107.13	499	Inland	Forest	Jul 1982-May 1993	Jan 1984-Dec 1992
Bratt's Lake	SK	50.20	-104.71	600	Inland	NA	Aug 2001-Dec 2010	Jan 2001-Dec 2011
McCreary	MB	50.71	-99.53	335	Inland	Agricultural	NA	Jan 1984-Dec 1995
Island Lake	MB	53.87	-94.67	245	Inland	Forest	NA	Jan 1984-Dec 1997
Experimental Lakes Area (ELA)	ON	49.66	-93.72	369	Inland	Forest	Jan 1979-Dec 2010	Jan 1984-Dec 2011
Pickle Lake B	ON	51.45	-90.22	370	Inland	Forest	NA	Jan 2003-Dec 2011
Algoma	ON	47.04	-84.38	411	Inland	Forest	Oct 1980-Dec 2010	Jan 1985-Dec 2011
Burnt Island	ON	45.82	-82.95	185	Inland	Forest	NA	Jan 1992-Dec 2011
Bonner Lake	ON	49.39	-82.12	245	Inland	Forest	short-term	Jun 1985-Dec 2011
Longwoods	ON	42.88	-81.48	239	Inland	Agricultural	Jan 1983-Dec 2010	Jan 1984-Dec 2011
Priceville	ON	44.17	-80.66	475	Inland	Agricultural	NA	Jan 1985-Dec 1994
Egbert	ON	44.23	-79.78	253	Inland	Agricultural	Jul 1988-Dec 2010	Jan 1989-Dec 2011
Egbert-2	ON	44.23	-79.78	253	Inland	Agricultural	short-term	Jan 1997-Dec 2011
Sprucedale	ON	45.42	-79.49	350	Inland	Agricultural	May 2002-Dec 2010	Jan 2003-Dec 2011
Warsaw Caves	ON	44.46	-78.13	230	Inland	Agricultural	NA	Jan 1986-Dec 2011
Chalk River	ON	46.06	-77.41	184	Inland	Forest	Jan 1979-Dec 2010	Jan 1984-Dec 2011
Chapais	QC	49.82	-74.98	381	Inland	Forest	Jun 1988-Dec 2010	Jan 1988-Dec 2011
Frelighsburg	QC	45.05	-72.86	203	Inland	Agricultural	Nov 2001-Dec 2010	Jan 2002-Dec 2011
Sutton	QC	45.08	-72.68	243	Inland	Forest	Jan 1986-Mar 2002	Jan 1984-Dec 2001
Lac Edouard	QC	47.68	-72.44	243	Inland	Forest	Jan 2002-Dec 2010	Jan 2002-Dec 2011
Montmorency	QC	47.32	-71.15	640	Coastal	Forest	Dec 1980-Jan 1997	Jan 1984-Dec 1996
Harcourt	NB	46.50	-65.27	37	Coastal	Forest	NA	Jan 1984-Dec 2011
Kejimkujik	NS	44.43	-65.21	127	Coastal	Forest	May 1979-Dec 2010	Jan 1984-Dec 2011
Mingan	QC	50.27	-64.22	14	Coastal	Forest	short-term	Jan 1994-Dec 2011
Jackson	NS	45.59	-63.84	90	Coastal	Forest	NA	Jan 1984-Dec 2011
Goose Bay	NL	53.31	-60.36	39	Coastal	Forest	NA	Jan 1984-Dec 2011
Goose Bay B	NL	53.29	-60.39	39	Coastal	Forest	NA	Jan 1989-Dec 2007
Bay d'Espoir	NL	47.99	-55.81	190	Coastal	Forest	short-term	Jan 1984-Dec 2011

Table 2: Rate of change in annual air concentrations. Slope refers to the Seasonal Kendall slope (ng m^{-3} a^{-1}); C.I. refers to the 90% confidence interval of the slope; ns indicates no significant trend; na indicates no available data.

Site	Ca^{2+}		Mg^{2+}		K^{+}		Na^{+}		Cl^{-}	
	Slope	C.I.	Slope	C.I.	Slope	C.I.	Slope	C.I.	Slope	C.I.
Saturna	-0.9	-1.3 to -0.6	-0.8	-1.1 to -0.4	-0.7	-1 to -0.5	-4.5	-6.5 to -1.8	1.0	ns
Esther	9.9	4.8 to 15.8	1.5	0.9 to 2.5	1.3	0.8 to 1.8	2.1	0.8 to 3.6	-0.4	-0.7 to 0
Cree Lake	na	na	na	na	-1.3	-2 to -0.5	0.5	ns	-0.5	-1 to -0.1
Bratt's Lake	5.5	ns	2.4	ns	-3.8	-5.3 to -2.4	-2.4	-4.2 to -1.3	-0.6	-1.3 to -0.2
ELA	0.5	ns	-0.2	ns	-0.5	-0.6 to -0.3	-0.7	-0.8 to -0.5	-0.2	-0.4 to -0.2
Algoma	-0.3	ns	-0.2	-0.5 to 0	-0.6	-0.8 to -0.5	-0.3	-0.5 to -0.2	-0.1	-0.2 to 0
Longwoods	-15.9	-21.1 to -10	-1.1	-2.1 to -0.4	-0.6	-0.9 to -0.3	-0.5	-0.8 to -0.2	-0.8	-1 to -0.5
Egbert	-9.7	-14.8 to -3.6	0.1	ns	0.02	ns	-0.2	ns	0.2	ns
Sprucedale	-2.7	ns	-0.9	ns	-1.2	-1.8 to -0.6	-1.3	-1.9 to -0.4	-0.2	ns
Chalk River	-0.3	ns	-0.6	-0.8 to -0.4	-0.8	-1 to -0.6	-0.5	-0.8 to -0.3	0.03	ns
Chapais	0.4	ns	-0.03	ns	-0.5	-0.6 to -0.4	-0.9	-1.2 to -0.7	0.3	0 to 0.6
Frelighsburg	-0.8	ns	0.3	ns	-1.1	-1.8 to -0.7	-2.6	-4.4 to -0.7	-0.01	ns
Sutton	1.5	ns	0.2	ns	-1.8	-2.3 to -1.4	-1.8	-2.3 to -1.4	-0.2	ns
Lac Edouard	-0.01	ns	-0.2	ns	-1.0	-1.4 to -0.6	-1.4	-2.1 to -0.5	-0.4	ns
Montmorency	na	na	na	na	-0.6	-1.1 to 0	1.4	0.8 to 2.1	0.1	ns
Kejimkujik	0.4	0 to 0.8	-0.5	-0.8 to -0.1	-0.5	-0.7 to -0.4	1.8	0.4 to 3	4.9	3.7 to 6.6

Site	NH_4^{+}		NO_3^{-}		SO_4^{2-}		SO_2		HNO_3	
	Slope	C.I.	Slope	C.I.	Slope	C.I.	Slope	C.I.	Slope	C.I.
Saturna	-7.6	-9.1 to -6.2	-9.3	-12.8 to -5.6	-28.8	-32.6 to -25.2	-62.6	-72.5 to -52.5	-17.1	-20.7 to -13.6
Esther	7.9	2 to 15.6	40.1	32.6 to 50.4	7.0	ns	-6.5	ns	12.0	2.2 to 21.8
Cree Lake	3.7	1.1 to 6.2	-1.1	ns	0.0	ns	8.4	ns	8.9	6 to 11.4
Bratt's Lake	-16.5	-23.4 to -9.7	-21.4	-34.3 to -10.5	-30.4	-51.1 to -11.8	1.6	ns	-19.4	-27.3 to -13.3
ELA	-4.4	-6 to -2.6	3.5	1.7 to 5.2	-28.4	-32.1 to -24.4	-14.6	-17.7 to -12.2	-2.3	-3.7 to -0.8
Algoma	-7.0	-9.9 to -3.7	6.4	4.4 to 8.4	-46.8	-55 to -39	-77.4	-87.2 to -67.3	-3.8	-7.1 to -0.9
Longwoods	-28.8	-34.4 to -23.1	-15.2	-22.9 to -6.5	-97.4	-110.2 to -87.4	-221.5	-240.2 to -202.1	-27.6	-32.7 to -23.3
Egbert	-41.8	-49.3 to -35.5	-34.2	-43.2 to -23.6	-93.9	-108.9 to -81.5	-199.4	-221.6 to -177.3	-25.1	-31.2 to -19.5
Sprucedale	-32.8	-52.4 to -12.6	-29.5	-39.9 to -16.6	-99.0	-150.5 to -36.8	-140.0	-188.7 to -97.2	-54.4	-74.5 to -36.3
Chalk River	-8.8	-11.6 to -6.4	2.8	1.5 to 4.3	-59.8	-66.9 to -52.1	-104.7	-115.3 to -94.1	-8.2	-10.8 to -5.7
Chapais	-5.7	-7 to -4.2	1.3	0.8 to 2	-41.3	-46.3 to -36	-45.5	-52.3 to -39.6	-4.3	-5.8 to -3.1
Frelighsburg	-58.2	-69 to -45.4	-53.4	-68.6 to -38.9	-108.6	-139.5 to -84	-160.8	-206 to -119.7	-81.7	-91.2 to -68.9
Sutton	-4.6	ns	18.8	13.9 to 24.2	-64.2	-80.4 to -51.2	-90.1	-112.8 to -67.3	-12.7	-18.9 to -4
Lac Edouard	-20.3	-27.9 to -13.1	-11.0	-14.3 to -6.4	-64.8	-88 to -47.6	-55.8	-76.2 to -34.1	-35.9	-42.4 to -27.1
Montmorency	9.6	6.1 to 14.6	5.9	4.5 to 8.2	-1.0	ns	-20.1	-40 to -3.2	21.0	14.9 to 29
Kejimkujik	-5.3	-6.5 to -4	2.5	1.4 to 3.8	-53.1	-59 to -47.5	-35.9	-41.2 to -30	-6.5	-7.9 to -4.8

Table 3: Rate of change in annual wet deposition of Ca^{2+}, Mg^{2+}, K^{+}, Na^{+}, and Cl^{-}. Slope refers to the Sen's slope (kg ha^{-1} a^{-1}); C.I. refers to the 90% confidence interval of the slope; ns indicates no significant trend.

Site	Ca^{2+}		Mg^{2+}		K^{+}		Na^{+}		Cl^{-}	
	Slope	C.I.	Slope	C.I.	Slope	C.I.	Slope	C.I.	Slope	C.I.
Saturna	0.001	ns	-0.0003	ns	-0.0002	ns	0.001	ns	0.002	ns
Esther	0.010	ns	0.003	ns	0.002	ns	0.002	ns	-0.001	ns
Cree Lake	-0.014	ns	-0.001	ns	-0.003	ns	0.001	ns	-0.002	ns
Bratt's Lake	0.036	ns	0.009	ns	0.005	ns	0.002	ns	0.001	ns
ELA	0.008	ns	0.002	ns	0.002	ns	-0.002	-0.004 to -0.0002	-0.001	ns
Algoma	-0.009	ns	-0.003	-0.0064 to -0.0005	-0.003	-0.0059 to -0.0003	-0.004	ns	-0.015	-0.025 to -0.01
Longwoods	-0.017	ns	-0.002	ns	0.006	0.003 to 0.011	0.004	ns	-0.013	-0.023 to -0.003
Egbert	0.003	ns	-0.001	ns	-0.0005	ns	0.004	0.002 to 0.009	-0.008	ns
Sprucedale	-0.024	ns	-0.008	-0.015 to -0.003	-0.002	ns	-0.005	ns	-0.037	ns
Chalk River	0.001	ns	-0.001	ns	-0.001	ns	0.001	ns	-0.008	-0.013 to -0.004
Chapais	0.004	ns	-0.001	-0.0022 to -0.0003	-0.0002	ns	-0.003	-0.006 to -0.001	-0.007	-0.012 to -0.002
Frelighsburg	0.020	ns	0.001	ns	0.001	ns	0.002	ns	-0.012	ns
Sutton	-0.029	-0.058 to -0.005	-0.002	ns	-0.001	ns	0.002	ns	-0.006	ns
Lac Edouard	-0.004	ns	-0.002	ns	-0.002	ns	-0.014	-0.022 to -0.001	-0.025	-0.046 to -0.008
Montmorency	-0.023	ns	-0.002	ns	0.001	ns	0.009	0.0009 to 0.016	0.006	ns
Kejimkujik	0.007	ns	0.003	ns	-0.0003	ns	0.024	ns	0.056	ns

Table 4: Rate of change in annual wet deposition of NH_4^+, NO_3^-, SO_4^{2-}, nss-SO_4^{2-}, precipitation amount and pH. Slope refers to the Sen's slope (kg ha^{-1} a^{-1}); C.I. refers to the 90% confidence interval of the slope; ns indicates no significant trend; na indicates no available data.

Site	NH_4^+		NO_3^-		SO_4^{2-}		nss-SO_4^{2-}		Annual precip (mm a^{-1})		pH (a^{-1})	
	Slope	C.I.	Slope	C.I.	Slope	C.I.	Slope	C.I.	Slope	C.I.	Slope	C.I.
Saturna	-0.01	ns	-0.07	-0.13 to -0.01	-0.13	-0.17 to -0.06	-0.12	-0.16 to -0.07	-1.5	ns	0.012	0.009 to 0.016
Esther	0.02	ns	0.04	ns	-0.02	ns	na	na	-1.4	ns	-0.012	ns
Cree Lake	-0.02	ns	-0.05	ns	-0.09	ns	na	na	-2.0	ns	-0.010	ns
Bratt's Lake	0.07	ns	0.02	ns	0.10	ns	na	na	25.9	ns	-0.009	ns
ELA	0.05	0.03 to 0.07	0.02	ns	-0.04	ns	na	na	6.0	ns	0.009	0.003 to 0.014
Algoma	-0.06	-0.09 to -0.02	-0.38	-0.51 to -0.26	-0.60	-0.71 to -0.47	na	na	-7.8	-14.5 to -2.7	0.020	0.016 to 0.025
Longwoods	0.03	ns	-0.33	-0.48 to -0.17	-0.55	-0.7 to -0.36	na	na	3.9	ns	0.023	0.019 to 0.028
Egbert	-0.001	ns	-0.31	-0.45 to -0.18	-0.45	-0.57 to -0.33	na	na	3.8	ns	0.027	0.022 to 0.03
Sprucedale	-0.03	ns	-1.01	-1.4 to -0.48	-1.00	-1.46 to -0.36	na	na	9.1	ns	0.030	0.018 to 0.042
Chalk River	0.01	ns	-0.19	-0.24 to -0.11	-0.36	-0.43 to -0.29	na	na	5.3	2.1 to 8.3	0.020	0.018 to 0.022
Chapais	-0.01	ns	-0.21	-0.28 to -0.11	-0.34	-0.45 to -0.25	na	na	-0.9	ns	0.015	0.013 to 0.018
Frelighsburg	-0.02	ns	-0.93	-1.29 to -0.64	-0.93	-1.57 to -0.16	na	na	13.5	ns	0.056	0.036 to 0.069
Sutton	0.05	0.01 to 0.09	0.01	ns	-0.57	-0.9 to -0.23	na	na	4.0	ns	0.017	0.01 to 0.026
Lac Edouard	-0.07	ns	-0.69	-0.91 to -0.38	-0.46	-0.77 to -0.23	na	na	14.6	ns	0.027	0.018 to 0.045
Montmorency	0.05	ns	0.20	ns	-0.27	ns	-0.27	ns	27.8	6.1 to 45.7	0.008	0.001 to 0.014
Kejimkujik	0.01	ns	-0.12	-0.18 to -0.06	-0.27	-0.37 to -0.2	-0.28	-0.36 to -0.2	10.9	3 to 17.2	0.014	0.011 to 0.017

Figure Captions

Figure 1: Geographical patterns of particulate inorganic ions and trace gas concentrations. Sites are arranged in order from western to eastern Canada. Grey shaded regions correspond to southern Ontario or southern Quebec sites. The blue line indicates the median; the red dot indicates the mean; the box and whiskers include the interquartile range and the 5^{th} to 95^{th} percentile range, respectively~~; the dotted line is the overall median among the sites~~. White boxes indicate 1983-1996 data and green boxes indicate 1997-2010 data (site labels also shown in green for this period).

Figure 2: Temporal trends of annual average atmospheric K^+ (a) and atmospheric NH_4^+ and annual ammonia emissions (b). In (b) between 2002 and 2010, atmospheric NH_4^+ at agricultural sites decreased by 6.3% while ammonia emissions in Ontario and Quebec decreased by 2.4% and 1.1%, respectively.

Figure 3: Temporal trends of annual atmospheric NO_3^- and annual NO_x emissions. Slope1 refers to the regression line for NO_3^- between 1991 and 2001 (positive trend, 3.6% increase), while Slope2 is for the period between 2001 and 2010 (negative trend, 6.5% decrease). Between 1991 and 1997, NOx emissions in Canada (Cdn) increased by 8.5%. Between 1997 and 2010, Cdn NOx emissions decreased by 25.8%.

Figure 4: Temporal trends of annual average atmospheric SO_4^- and annual SO_2 emissions. ON and QC refer to the province of Ontario and Quebec, respectively. Between 1990 and 2010, atmospheric SO_4^- decreased by 4.5% at southern Ontario (ON) and Quebec (QC) sites and by 3.6% at other sites. Over the same period, SO_2 emissions decreased by 1.8% in Canada (Cdn) and 4.3% in the U.S.

Figure 5: Geographical patterns of cation/anion (c/a) ratio (a) and temporal trends of annual average c/a ratio and precipitation pH (b). In (a), the blue line indicates the median; the red dot indicates the mean; the box and whiskers include the interquartile range and the 5^{th} to 95^{th} percentile range, respectively; the dotted line is the overall median among the sites.

Figure 6: Geographical patterns of the annual wet deposition of ions. Sites are arranged in order from western to eastern Canada. The blue line indicates the median; the red dot indicates the mean; the box and whiskers include the interquartile range and the 5^{th} to 95^{th} percentile range, respectively; the dotted line is the overall median among the sites.

Figure 7: Temporal trends of annual wet deposition of Cl^- and NO_3^- (a) and SO_4^{2-} (b).

Figure 8: Geographical patterns of precipitation pH. See Fig. 6 caption.

Figure 9: Average percent contributions of gas and particulate-phase species to nitrate (a), ammonium (b), and sulfate (c) wet deposition.

Figure 10: Monthly variation in the contributions of gas and particulate-phase species to nitrate (a), ammonium (b), and sulfate (c) wet deposition. Error bars represent the standard deviation of the percent contributions by gas and particulate-phase species between sites.

Fig. 1

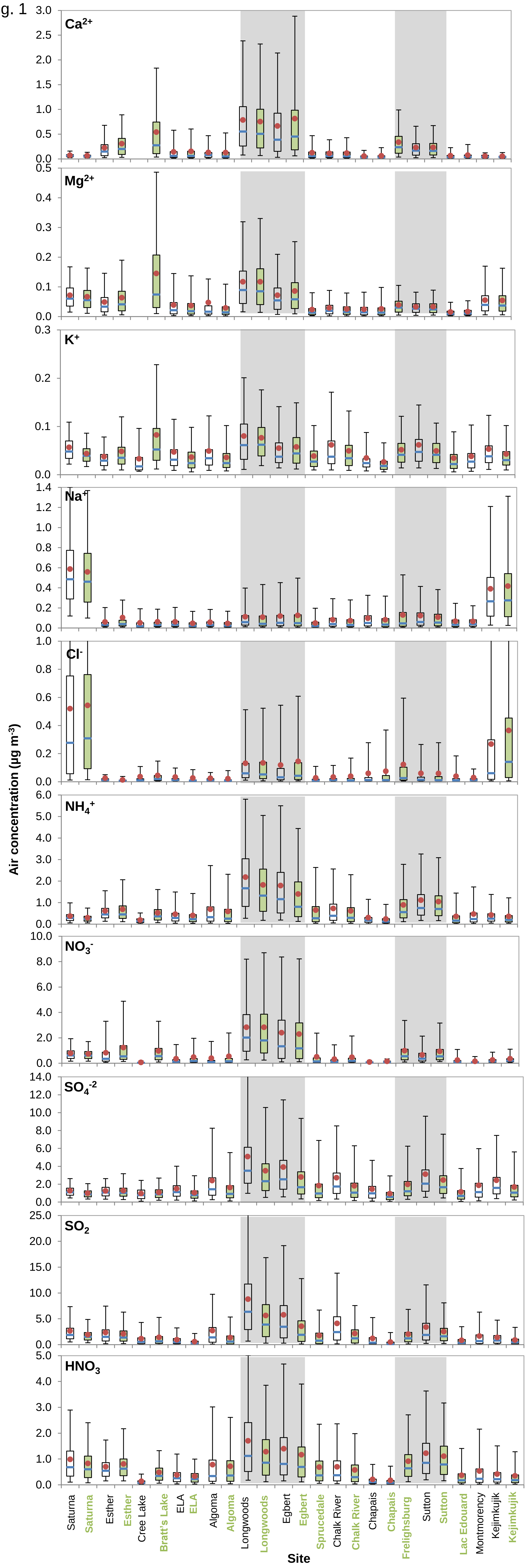

Ca2+
Mg2+
K+
Na+
Cl-
NH4+
NO3-
SO4-2
SO2
HNO3
Air concentration (μg m-3)
Saturna
Saturna
Esther
Esther
Cree Lake
Bratt's Lake
ELA
ELA
Algoma
Algoma
Longwoods
Longwoods
Egbert
Egbert
Sprucedale
Chalk River
Chalk River
Chapais
Chapais
Frelighsburg
Sutton
Sutton
Lac Edouard
Montmorency
Kejimkujik
Kejimkujik
Site

Fig. 2

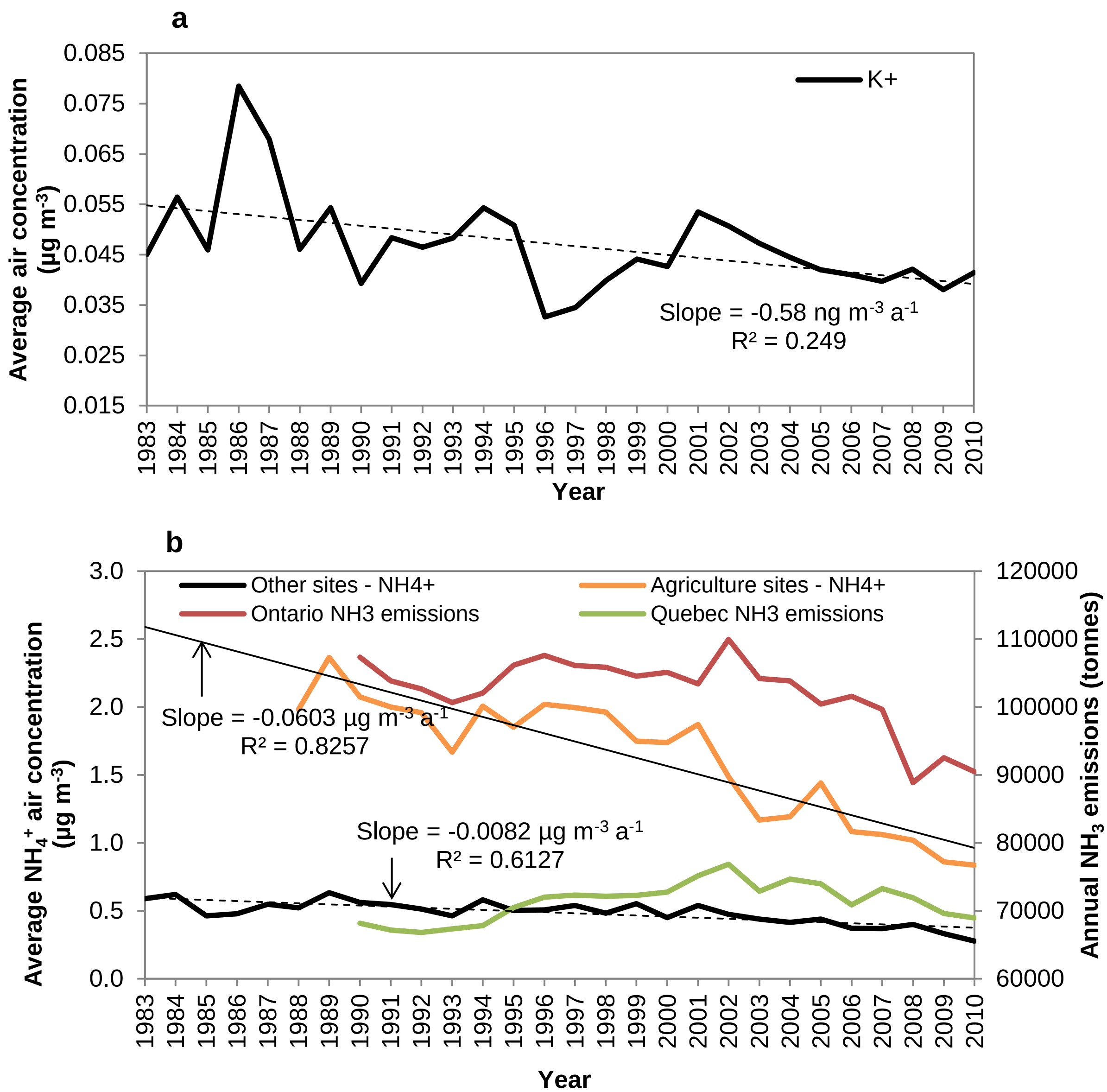
a
K+
Slope = -0.58 ng m-3 a-1
R² = 0.249
Average air concentration (µg m-3)
Year
b
Other sites - NH4+
Agriculture sites - NH4+
Ontario NH3 emissions
Quebec NH3 emissions
Slope = -0.0603 µg m-3 a-1
R² = 0.8257
Slope = -0.0082 µg m-3 a-1
R² = 0.6127
Average NH4+ air concentration (µg m-3)
Annual NH3 emissions (tonnes)
Year

Fig. 3

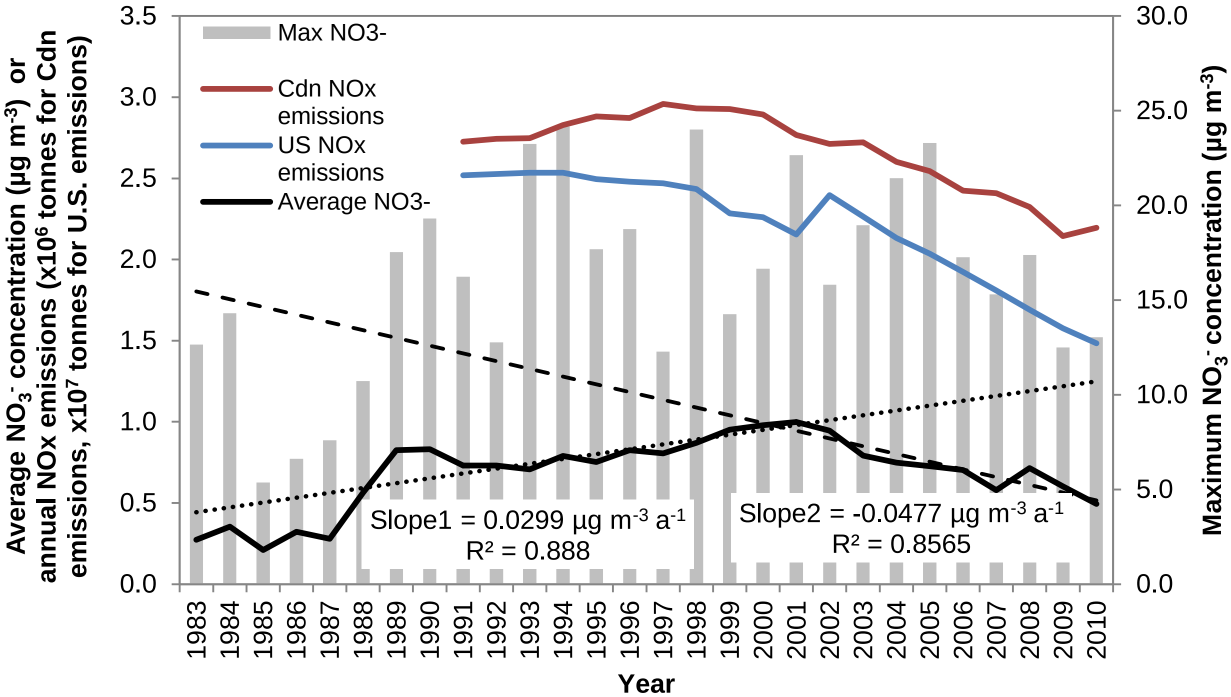

Max NO3-
Cdn NOx emissions
US NOx emissions
Average NO3-
Slope1 = 0.0299 µg m-3 a-1
R² = 0.888
Slope2 = -0.0477 µg m-3 a-1
R² = 0.8565
Average NO3- concentration (µg m-3) or annual NOx emissions (x10^6 tonnes for Cdn emissions, x10^7 tonnes for U.S. emissions)
Maximum NO3- concentration (µg m-3)
Year
3.5
3.0
2.5
2.0
1.5
1.0
0.5
0.0
30.0
25.0
20.0
15.0
10.0
5.0
0.0
1983
1984
1985
1986
1987
1988
1989
1990
1991
1992
1993
1994
1995
1996
1997
1998
1999
2000
2001
2002
2003
2004
2005
2006
2007
2008
2009
2010

Fig. 4

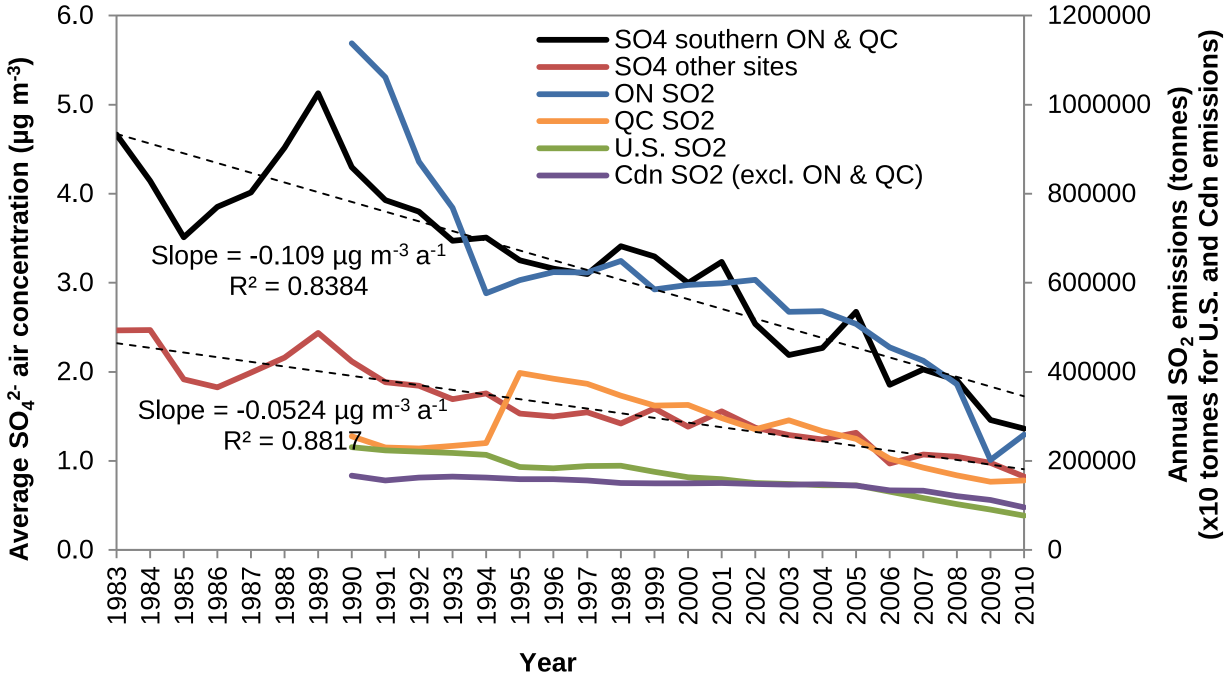

SO4 southern ON & QC
SO4 other sites
ON SO2
QC SO2
U.S. SO2
Cdn SO2 (excl. ON & QC)
Slope = -0.109 µg m-3 a-1
R² = 0.8384
Slope = -0.0524 µg m-3 a-1
R² = 0.8817
Average SO4 2- air concentration (µg m-3)
Annual SO2 emissions (tonnes)
(x10 tonnes for U.S. and Cdn emissions)
Year
0.0
1.0
2.0
3.0
4.0
5.0
6.0
0
200000
400000
600000
800000
1000000
1200000
1983
1984
1985
1986
1987
1988
1989
1990
1991
1992
1993
1994
1995
1996
1997
1998
1999
2000
2001
2002
2003
2004
2005
2006
2007
2008
2009
2010

Fig. 5

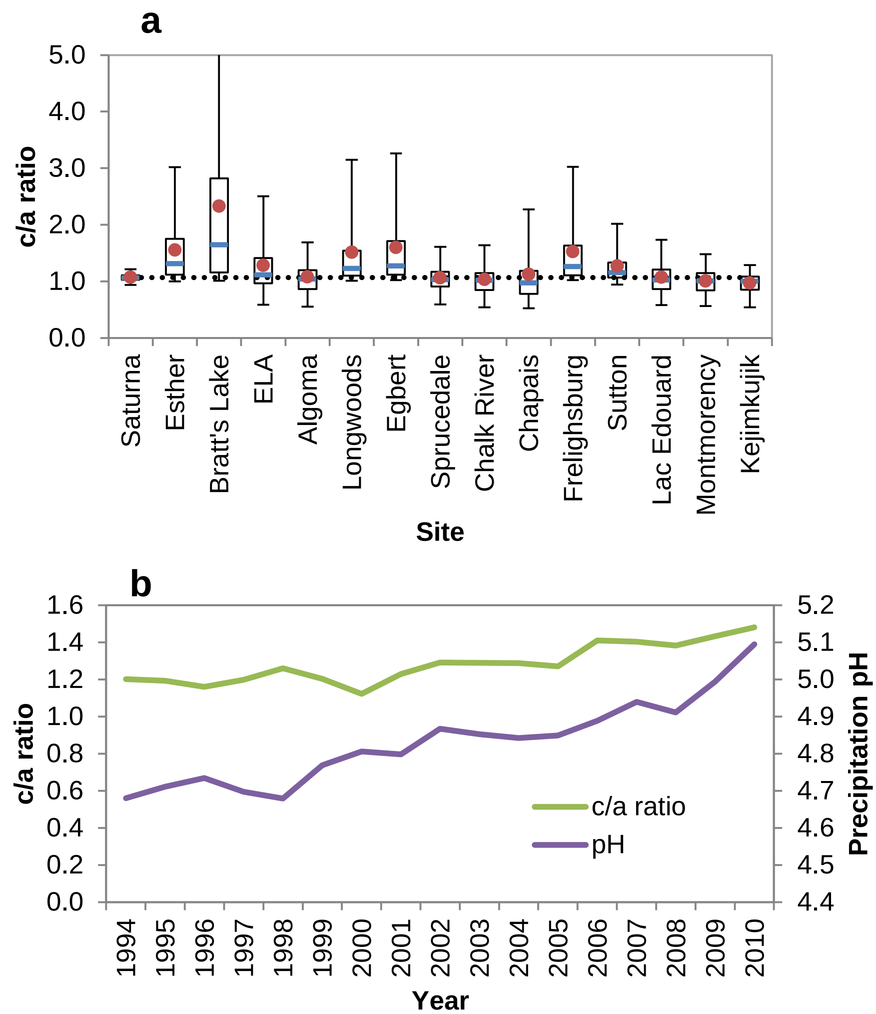
a
5.0
4.0
3.0
2.0
1.0
0.0
c/a ratio
Saturna
Esther
Bratt's Lake
ELA
Algoma
Longwoods
Egbert
Sprucedale
Chalk River
Chapais
Frelighsburg
Sutton
Lac Edouard
Montmorency
Kejimkujik
Site
b
1.6
1.4
1.2
1.0
0.8
0.6
0.4
0.2
0.0
c/a ratio
5.2
5.1
5.0
4.9
4.8
4.7
4.6
4.5
4.4
Precipitation pH
c/a ratio
pH
1994
1995
1996
1997
1998
1999
2000
2001
2002
2003
2004
2005
2006
2007
2008
2009
2010
Year

Fig. 6

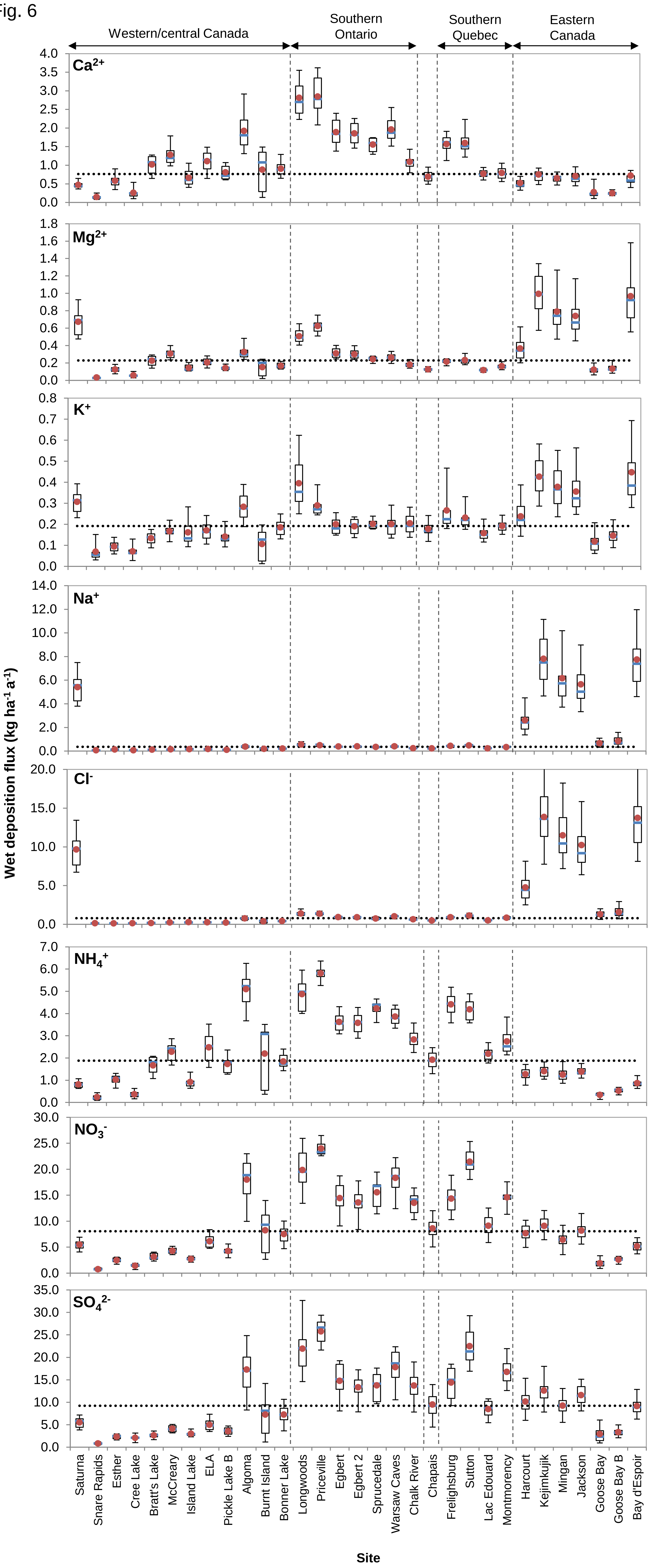

Western/central Canada
Southern Ontario
Southern Quebec
Eastern Canada
Ca^{2+}
Mg^{2+}
K^{+}
Na^{+}
Cl^{-}
NH_4^{+}
NO_3^{-}
SO_4^{2-}
Wet deposition flux (kg ha^{-1} a^{-1})
Saturna
Snare Rapids
Esther
Cree Lake
Bratt's Lake
McCreary
Island Lake
ELA
Pickle Lake B
Algoma
Burnt Island
Bonner Lake
Longwoods
Priceville
Egbert
Egbert 2
Sprucedale
Warsaw Caves
Chalk River
Chapais
Frelighsburg
Sutton
Lac Edouard
Montmorency
Harcourt
Kejimkujik
Mingan
Jackson
Goose Bay
Goose Bay B
Bay d'Espoir
Site

Fig. 7

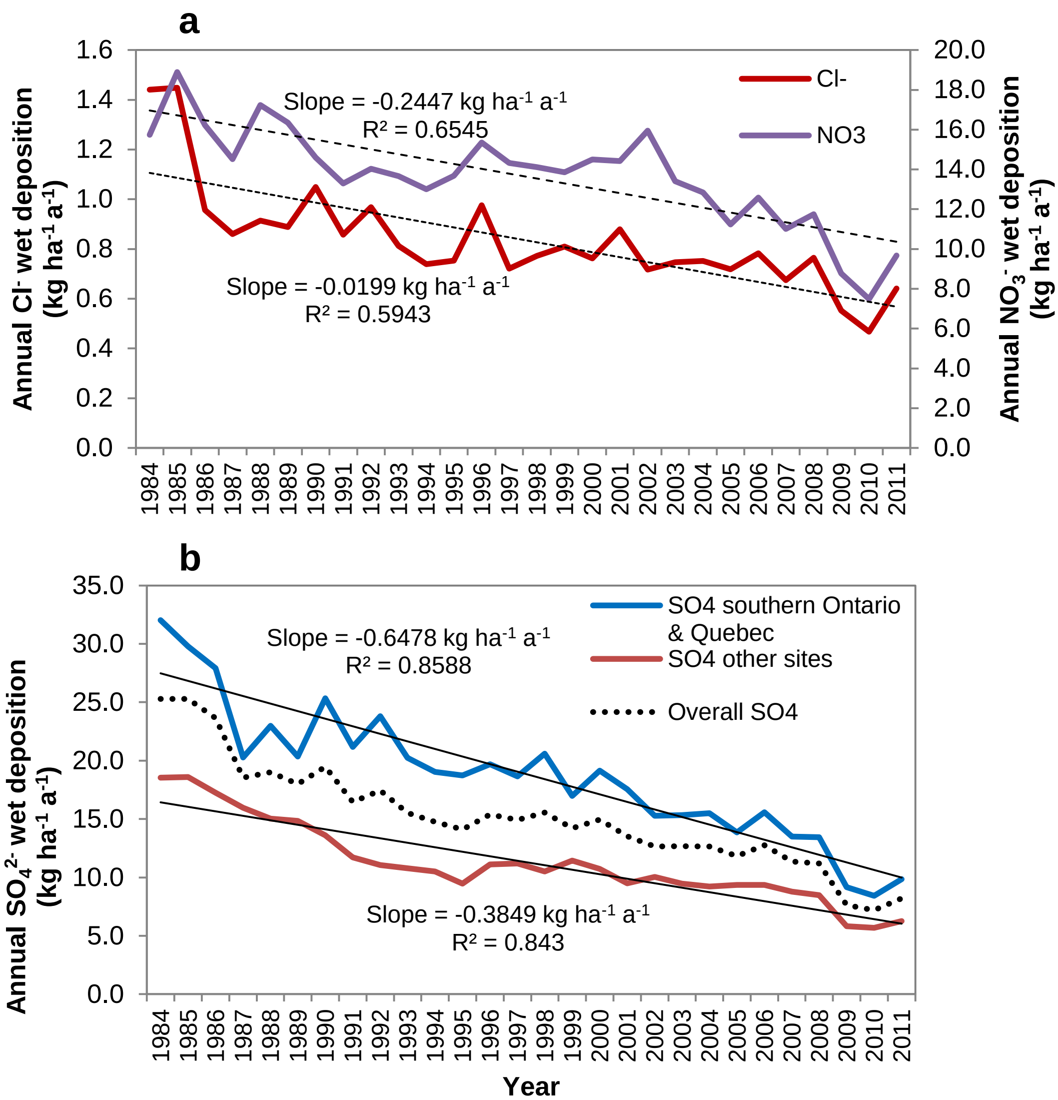

a
Annual Cl⁻ wet deposition (kg ha⁻¹ a⁻¹)
Annual NO₃⁻ wet deposition (kg ha⁻¹ a⁻¹)
Cl-
NO3
Slope = -0.2447 kg ha⁻¹ a⁻¹
R² = 0.6545
Slope = -0.0199 kg ha⁻¹ a⁻¹
R² = 0.5943
b
Annual SO₄²⁻ wet deposition (kg ha⁻¹ a⁻¹)
SO4 southern Ontario & Quebec
SO4 other sites
Overall SO4
Slope = -0.6478 kg ha⁻¹ a⁻¹
R² = 0.8588
Slope = -0.3849 kg ha⁻¹ a⁻¹
R² = 0.843
Year

Fig. 8

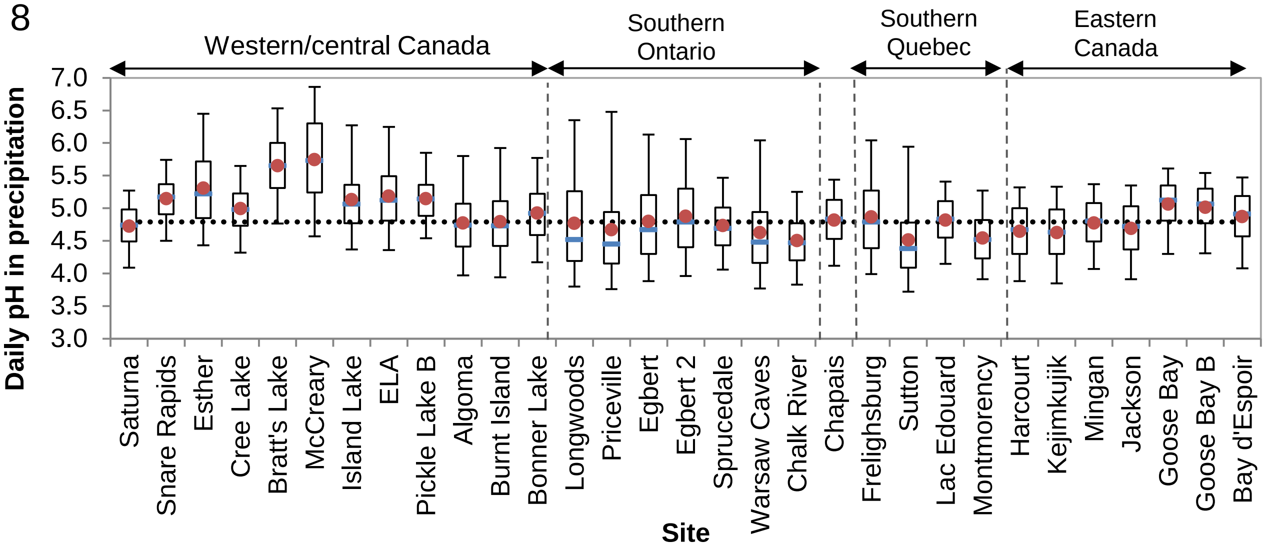
Western/central Canada
Southern Ontario
Southern Quebec
Eastern Canada
Daily pH in precipitation
7.0
6.5
6.0
5.5
5.0
4.5
4.0
3.5
3.0
Saturna
Snare Rapids
Esther
Cree Lake
Bratt's Lake
McCreary
Island Lake
ELA
Pickle Lake B
Algoma
Burnt Island
Bonner Lake
Longwoods
Priceville
Egbert
Egbert 2
Sprucedale
Warsaw Caves
Chalk River
Chapais
Frelighsburg
Sutton
Lac Edouard
Montmorency
Harcourt
Kejimkujik
Mingan
Jackson
Goose Bay
Goose Bay B
Bay d'Espoir
Site

Fig. 9

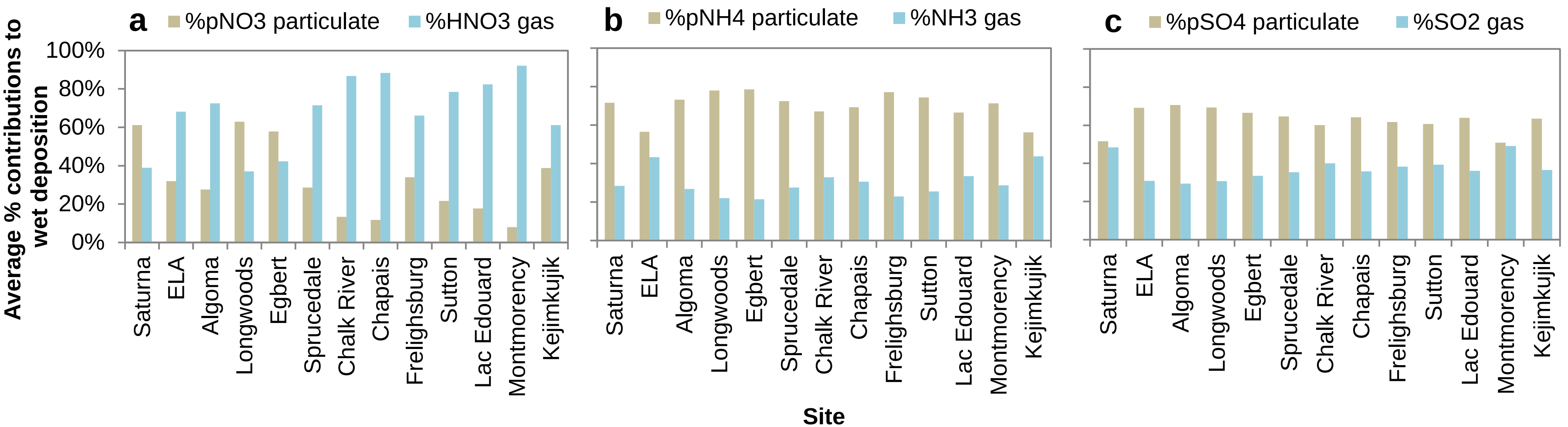

a
%pNO3 particulate
%HNO3 gas
b
%pNH4 particulate
%NH3 gas
c
%pSO4 particulate
%SO2 gas
Average % contribution to wet deposition
100%
80%
60%
40%
20%
0%
Saturna
ELA
Algoma
Longwoods
Egbert
Sprucedale
Chalk River
Chapais
Frelighsburg
Sutton
Lac Edouard
Montmorency
Kejimkujik
Site

Fig. 10

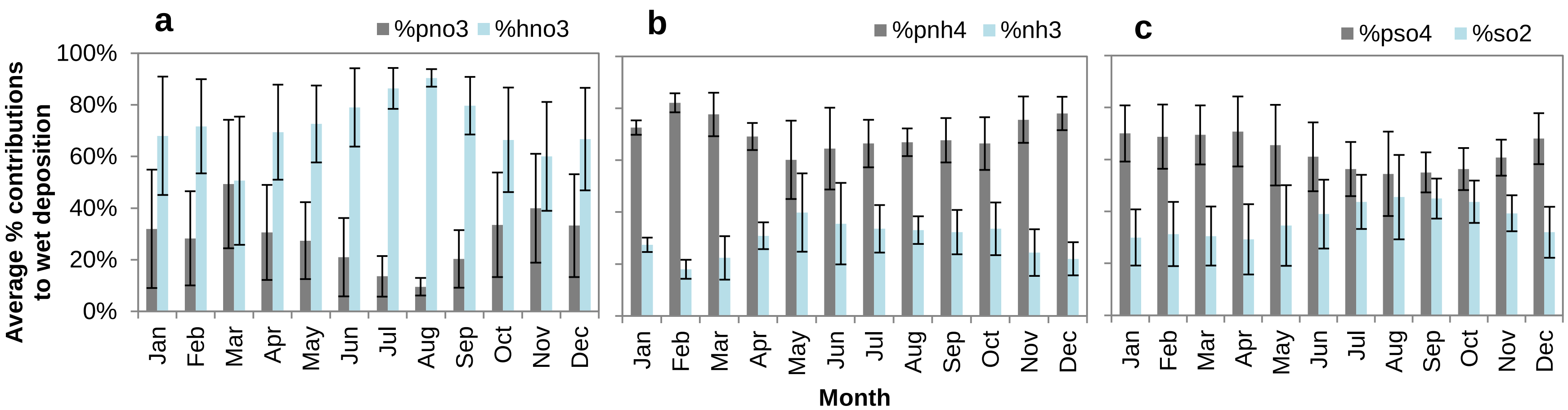
a
%pno3
%hno3
b
%pnh4
%nh3
c
%pso4
%so2
100%
80%
60%
40%
20%
0%
Average % contribution to wet deposition
Jan
Feb
Mar
Apr
May
Jun
Jul
Aug
Sep
Oct
Nov
Dec
Month

Supplementary Material

Long-term air concentrations, wet deposition, and scavenging ratios of inorganic ions, HNO_3 and SO_2 and assessment of aerosol and precipitation acidity at Canadian rural locations

Irene Cheng and Leiming Zhang
Air Quality Research Division, Science and Technology Branch, Environment and Climate Change Canada, 4905 Dufferin Street, Toronto, Ontario, M3H 5T4, Canada

Correspondence to: Irene Cheng (irene.cheng@canada.ca)

Section S1: Correlation analysis between particulate ions and meteorological variables

The influence of meteorological parameters including temperature, relative humidity and precipitation rates on the temporal trends of particulate ions and trace gases were also investigated by performing correlation analyses on the monthly averaged data. The descending trend in K^+ between 1993 and 2010 at the majority of the sites was not strongly influenced by precipitation as evident by the weak correlation coefficients (Table S1). Higher correlation between monthly average K^+ and temperature were found at Sprucedale, Frelighsburg and Lac Edouard ($r = 0.52$-0.69, $p<0.05$). At these sites, the monthly average K^+ peaked in March-April and was at the minimum concentration during December-January, which resembled the seasonal temperature cycle (Fig. S2a). The higher K^+ in the early spring could be attributed to increase soil emissions from agriculture operations and forest fires during springtime since the major sources of particulate K^+ are from biomass and soil. Decreasing NH_4^+ observed at most of the sites was only weakly correlated with monthly precipitation rates and relative humidity, implying these meteorological parameters had little influence on the long-term temporal trend. Higher correlation between monthly average NH_4^+ and temperature was found at Kejimkujik ($r = 0.63$, $p<0.05$). The maximum NH_4^+ typically occurred during April-May and reached its lowest concentration during December-January (Fig. S2b). This seasonal trend is linked to the formation of SO_4^{2-} through SO_2 oxidation, which tends to occur at higher temperatures because of increase production of atmospheric oxidants. This theory is consistent with the very high correlation between monthly average NH_4^+ and SO_4^{2-} ($r = 0.91$, $p<0.05$) at Kejimkujik. Overall, strong correlations between NH_4^+ and SO_4^{2-} were observed at all the sites ($r = 0.6$-0.94, $p<0.05$). The high correlation between SO_4^{2-}/SO_2 ratio and temperature ($r = 0.61$-0.84, $p<0.05$) suggests SO_4^{2-} formation from the gas-phase oxidation of SO_2 (Yao et al., 2002). Besides the relationship between NH_4^+ and SO_4^{2-}, three of the sites including Saturna, ELA and Egbert exhibited strong correlations between NH_4^+ and NO_3^- ($r = 0.52$-0.7, $p<0.05$) indicating that NH_4^+ also followed the temporal trend of NO_3^- at some locations. In summary, precipitation and relative humidity had little impact on the long-term temporal patterns of particulate ions. Seasonal temperature trends ~~is~~ are linked with the seasonal cycle of atmospheric oxidants which explains the short-term patterns in SO_4^{2-} and NH_4^+~~;~~. ~~however, there is no clear evidence that~~ However, the correlation analysis using monthly data did not find a strong relationship between long-term temperature changes and long-term trends in SO_4^{2-} and NH_4^+ concentrations. The lack of trends is related to the combined effects of increasing temperature and decreasing sulfur dioxide emissions. Studies suggest an increase in temperature would increase ammonia emissions and the partitioning of ammonium nitrate to ammonia (Sutton et al., 2013; Yao and Zhang, 2016). However, the decreasing trend in sulfur dioxide emissions would likely reduce atmospheric sulfate and subsequently lead to lower ammonium sulfate production (Yao and Zhang, 2016).

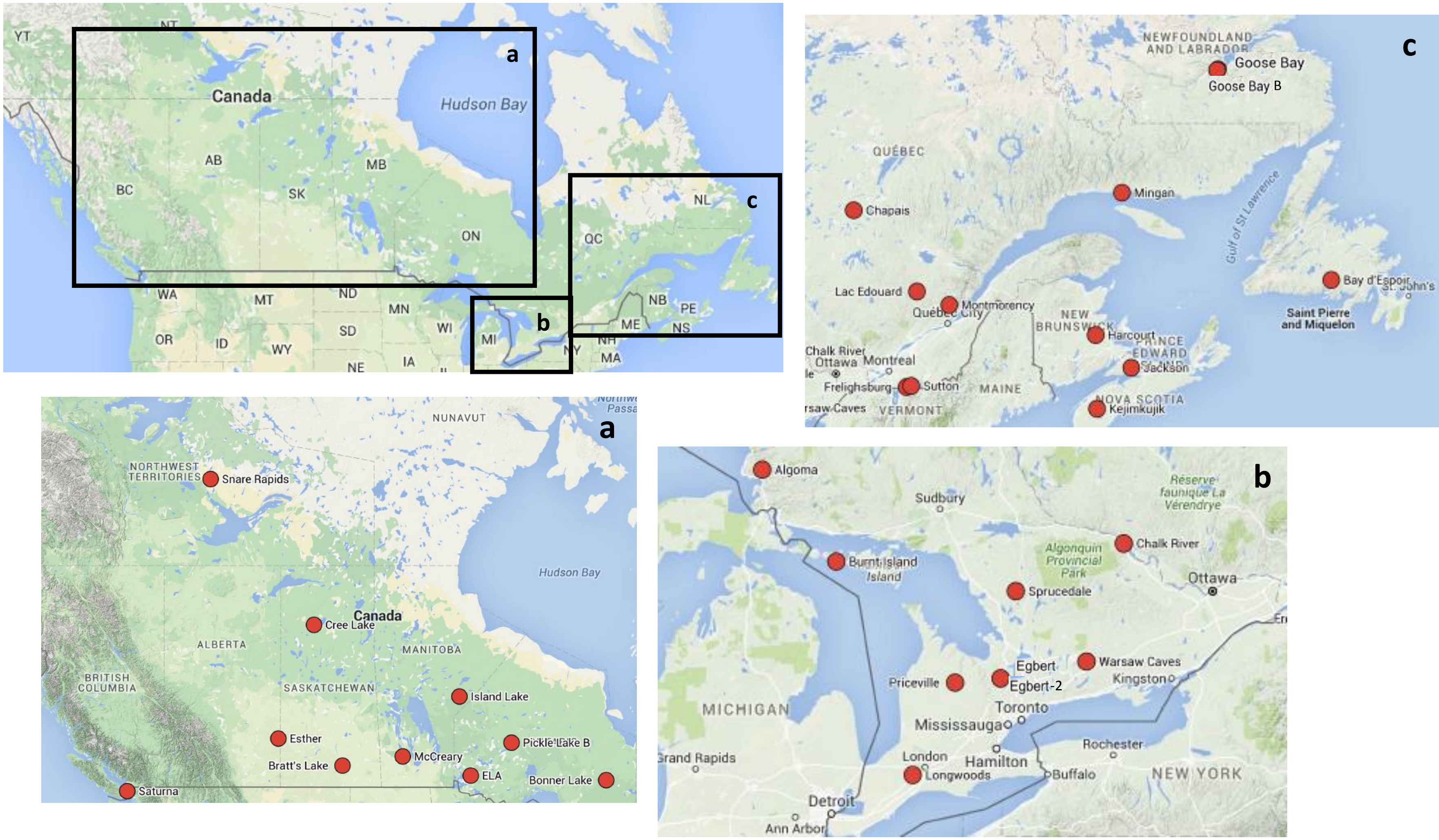

Figure S1: Map of ~~30~~ 31 CAPMoN sites in western/central Canada (a), southern Ontario (b), and Quebec and eastern Canada (c).

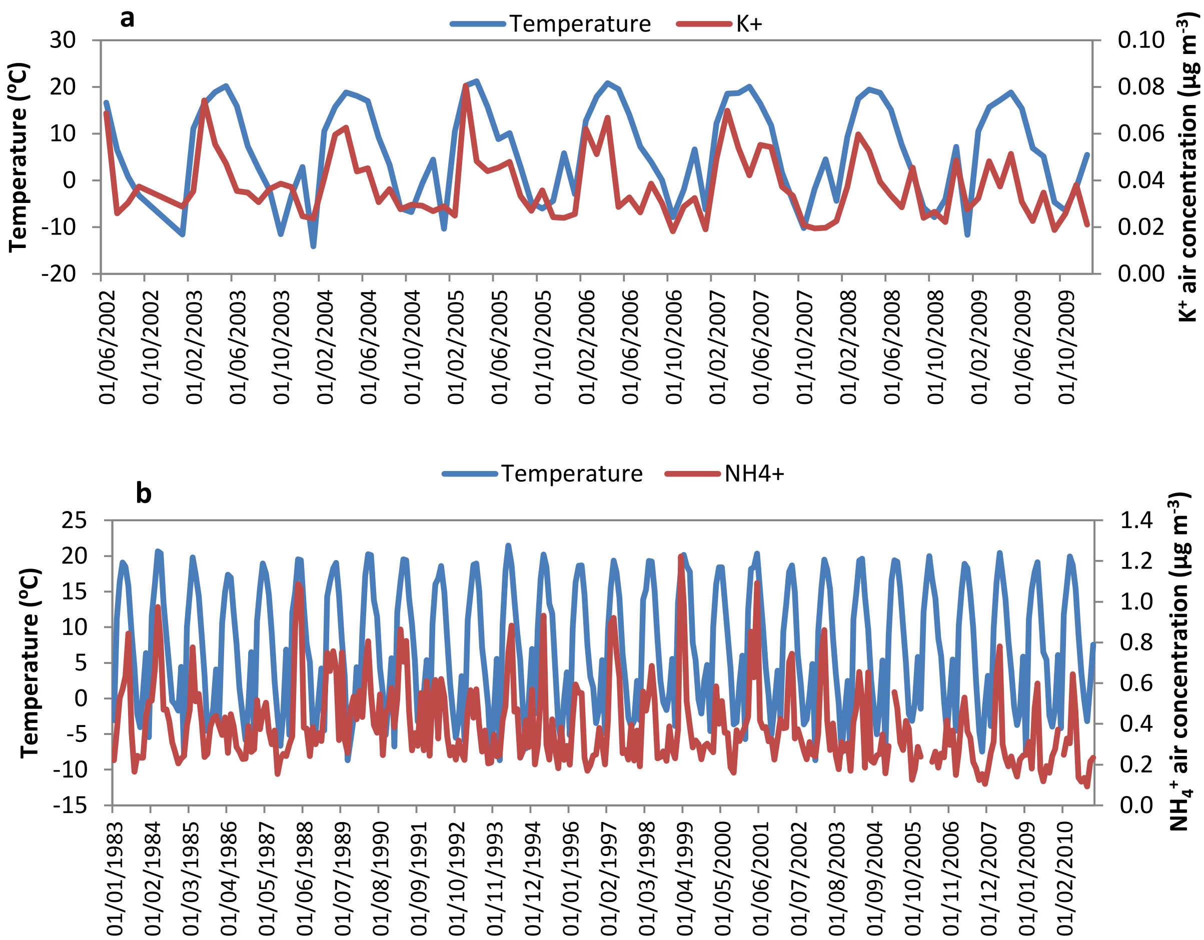

Figure S2: Time-series plots of monthly average air temperature and atmospheric K^+ from Sprucedale, Frelighsburg and Lac Edouard (combined) (a) and monthly average air temperature and atmospheric NH_4^+ at Kejimkujik (b).

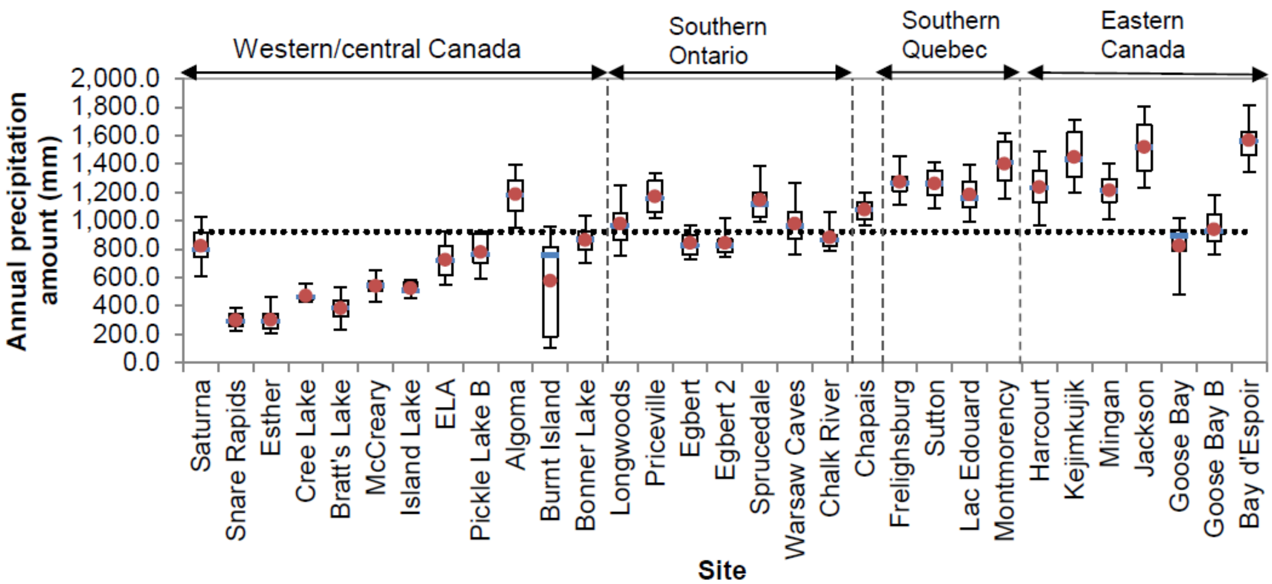

Figure S3: Geographical pattern of the annual precipitation amount. The blue line indicates the median; the red dot indicates the mean; the box and whiskers include the interquartile range and the 5th to 95th percentile range, respectively; the dotted line is the overall median among the sites.

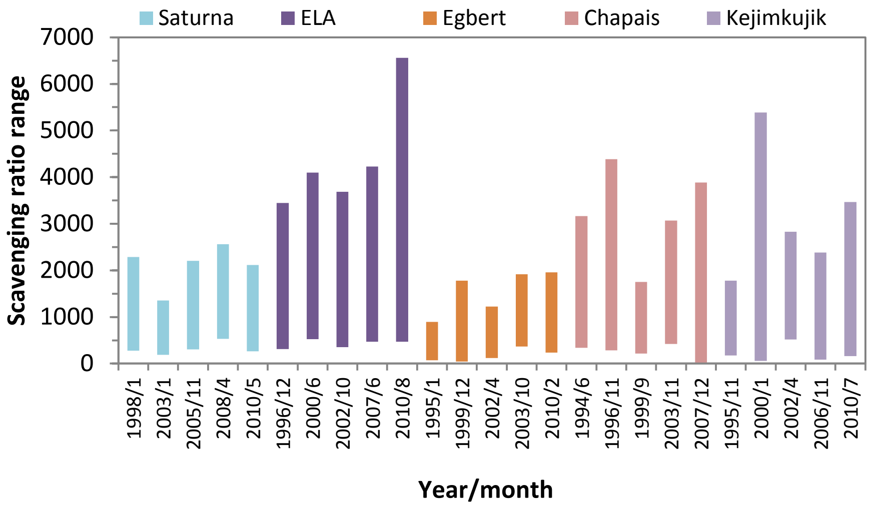

Figure S4: Variability in scavenging ratios among different inorganic ions and trace gases within the same month for five different years at five of the sites.

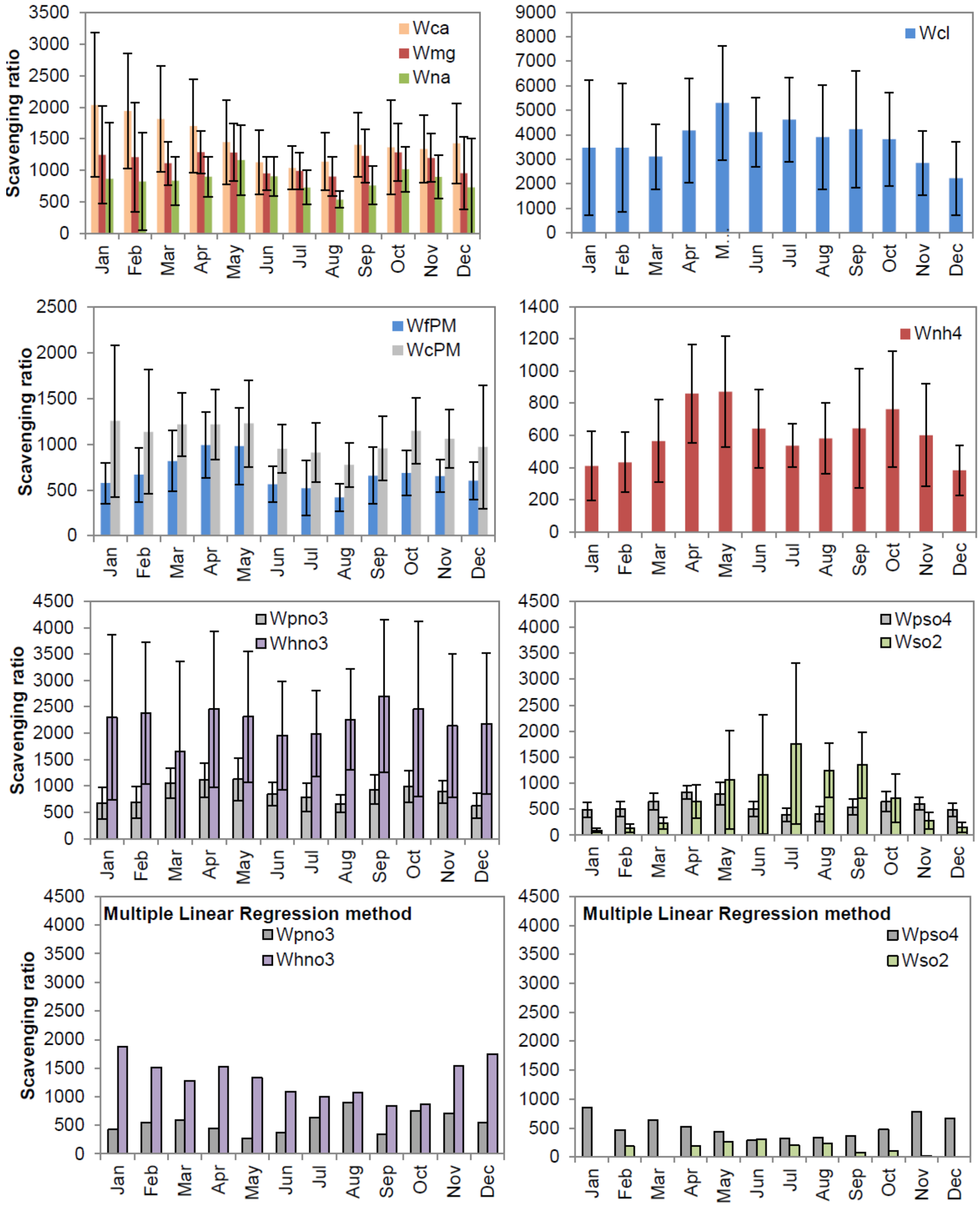

Figure S5: Monthly variation in scavenging ratios among 13 sites. Error bars represent the standard deviation of scavenging ratios between sites. W_{fPM} and W_{cPM} are the fine and coarse particle scavenging ratios, respectively.

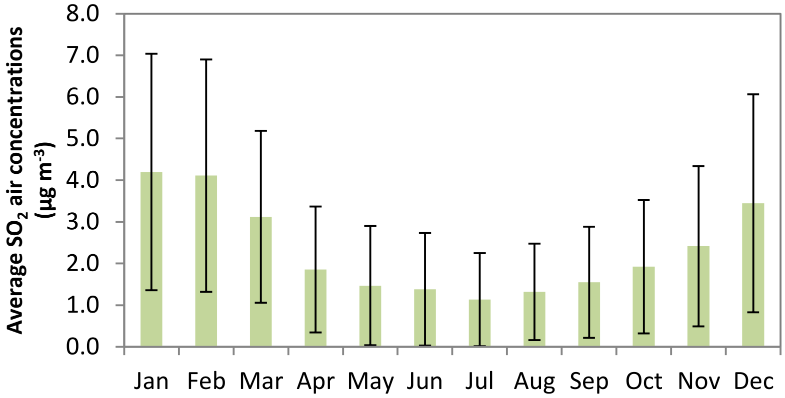

Figure S6. Monthly variation in SO_2 air concentrations. Error bars represent the standard deviation between sites.

Table S1: Pearson correlation coefficients between selected ions and meteorological parameters (significant at $p<0.05$; otherwise non-significant (ns)). Note that the ion concentrations and meteorological parameters are monthly averages.

	K^+			NH_4^+					SO_4^{2-}/SO_2
Site	Temp	RH	Precip	Temp	RH	Precip	NO_3^-	SO_4^{2-}	Temp
Saturna	-0.20	0.18	0.18	-0.04^{ns}	-0.23	-0.17	0.67	0.60	0.61
Bratt's Lake	0.09^{ns}	-0.20	-0.25						
ELA	0.20	-0.03^{ns}	0.12	-0.26	0.13	-0.22	0.70	0.78	0.75
Algoma	0.42	-0.07^{ns}	-0.04^{ns}	0.36	0.10	-0.17	0.23	0.87	0.73
Longwoods				-0.05^{ns}	0.20	-0.06^{ns}	0.44	0.68	0.81
Egbert				-0.07^{ns}	0.03^{ns}	-0.21	0.52	0.75	0.77
Sprucedale	0.69	0.05^{ns}	-0.14^{ns}	0.30	0.06^{ns}	-0.23	0.20^{ns}	0.92	0.73
Chalk River	0.31	-0.005^{ns}	0.05^{ns}	0.37	0.09	0.02^{ns}	0.10^{ns}	0.85	0.64
Chapais	0.41	-0.17	0.18	0.38	-0.21	0.04^{ns}	0.23	0.85	0.77
Frelighsburg	0.53	0.08^{ns}	0.13^{ns}	0.11^{ns}	0.13^{ns}	-0.13^{ns}	0.36	0.86	0.84
Lac Edouard	0.52	-0.15^{ns}	0.21	0.34	0.01^{ns}	0.11^{ns}	0.23	0.94	0.76
Kejimkujik	0.31	-0.17	-0.15	0.63	-0.30	-0.32	-0.16	0.91	0.83

Table S2: Average cation and anion concentrations (neq m^{-3}) in particulate matter by site and year

Site	Cation	Anion		Year	Cation	Anion
Saturna	0.047	0.045		1994	0.074	0.066
Esther	0.052	0.033		1995	0.071	0.063
Bratt's Lake	0.060	0.031		1996	0.073	0.063
ELA	0.024	0.024		1997	0.073	0.063
Algoma	0.024	0.028		1998	0.076	0.064
Longwoods	0.133	0.108		1999	0.075	0.066
Egbert	0.096	0.072		2000	0.067	0.062
Sprucedale	0.024	0.024		2001	0.078	0.068
Chalk River	0.028	0.034		2002	0.073	0.061
Chapais	0.016	0.019		2003	0.065	0.055
Frelighsburg	0.060	0.043		2004	0.063	0.054
Sutton	0.062	0.054		2005	0.069	0.059
Lac Edouard	0.016	0.018		2006	0.058	0.046
Montmorency	0.023	0.026		2007	0.058	0.048
Kejimkujik	0.035	0.041		2008	0.060	0.048
				2009	0.052	0.041
				2010	0.048	0.037

Table S3: Scavenging ratio (W) statistics from this study (mass basis). na indicates no available data. "C" indicates coastal locations.

Site	W_{Ca2+}	W_{Mg2+}	W_{Na+}	$W_{coarsePM}$	$W_{finePM} = W_k$	W_{Cl}	W_{NH4}	W_{pNO3}	W_{HNO3}	W_{pSO4}	W_{SO2}
Mean											
Saturna[C]	1671	1493	1390	1505	567	2103	445	897	776	602	233
ELA	1893	1347	1208	1496	885	3519	848	1224	3079	696	1247
Algoma	2413	1510	1002	1426	911	5779	762	1204	2064	734	330
Longwoods	911	901	865	881	996	2011	303	657	749	601	125
Egbert	625	748	713	697	554	1914	283	583	982	473	181
Sprucedale	1822	1299	905	1342	611	4278	577	998	2012	611	445
Chalk River	na	na	666	666	580	5065	466	632	3005	547	560
Chapais	2077	899	475	1043	758	1855	625	932	5527	661	1291
Frelighsburg	852	838	647	781	553	2554	411	642	1375	471	414
Sutton	1010	936	594	753	497	4377	350	631	1616	473	396
Lac Edouard	1702	1105	577	1128	512	3192	465	842	2398	496	771
Montmorency	1200	1148	599	742	607	4969	406	697	2201	471	1222
Kejimkujik[C]	1729	1980	2120	2077	702	4959	303	1120	1842	571	1339
Max avg/min avg ratio	3.9	2.6	4.5	3.1	2.0	3.1	3.0	2.1	7.4	1.6	10.7
Median											
Saturna[C]	1552	1404	1245	1430	502	1934	416	796	650	533	208
ELA	1395	1141	993	1358	765	3235	726	1151	2711	628	1141
Algoma	1946	1266	816	1272	769	4532	655	1046	1880	698	203
Longwoods	840	832	775	802	682	1684	252	601	857	531	60
Egbert	535	693	585	635	440	1355	245	521	829	428	127
Sprucedale	1504	1238	765	1218	556	3872	582	945	1906	582	204

Chalk River	na	na	531	531	437	4321	401	526	2568	449	284
Chapais	1743	712	363	883	640	1216	544	787	4914	578	828
Frelighsburg	774	754	540	742	438	1788	405	599	1322	442	251
Sutton	968	888	549	706	445	2972	314	562	1452	435	241
Lac Edouard	1483	1015	497	1023	450	2480	380	780	2077	404	453
Montmorency	1130	833	474	623	432	3633	347	559	2173	386	809
Kejimkujik[C]	1482	1416	1447	1452	541	3511	279	926	1571	488	461
Max median/min median ratio	3.6	2.0	4.0	2.7	1.8	3.7	3.0	2.2	7.6	1.8	19.0
Standard deviation											
Saturna[C]	798	727	734	655	271	1001	217	381	547	276	123
ELA	1684	810	1016	990	483	2159	476	680	1636	336	880
Algoma	1869	1061	661	973	653	5161	517	753	1017	284	372
Longwoods	439	398	362	312	869	1331	159	233	453	273	142
Egbert	373	317	427	322	501	1547	170	307	647	214	180
Sprucedale	1039	634	637	597	286	2940	253	504	840	259	523
Chalk River	na	na	450	450	417	3763	313	392	1629	352	681
Chapais	1273	668	349	641	407	1969	328	529	2654	339	1373
Frelighsburg	415	367	382	331	514	2288	157	311	523	170	438
Sutton	374	371	254	302	321	3320	155	284	618	234	445
Lac Edouard	1003	597	361	517	281	2188	257	412	1195	260	843
Montmorency	628	783	354	441	478	4489	231	425	960	324	1151
Kejimkujik[C]	1134	1643	1942	1823	671	4723	154	687	1172	391	2245

Table S4: Scavenging ratios from literature (mass basis). * Most literature values excluded gas scavenging except where indicated; [1]Derived from multiple linear regression; [2]Wp_{NO3} based on sum of pNO_3^- and HNO_3 in air; [3]W_{pSO4} based on sum of pSO_4^{2-} andSO_2 in air; [4]Snow events only.

Location	W_{Ca2+}	W_{Mg2+}	W_{Na+}	W_{K+}	W_{Cl}	$*W_{NH4}$	$*W_{pNO3}$	$*W_{pSO4}$	W_{HNO3}	W_{SO2}	Reference
CAPMoN sites, Canada	625-2413	748-1980	475-2120	497-996	1855-5779	283-848	583-1224	471-734	749-5527	125-1339	This study
							523-1776	391-903	722-2848	31-409	This study[1]
Eastern Canada							832-2950	831-1550			Barrie et al. (1985)[2]
NADP/CASTNET sites, U.S.	860-2526	656-2011	798-7409	265-885	1430-22950						Cheng et al. (2015)
NADP/AIRMoN sites, U.S.						96-3050		216-2710	300-1700		Hicks (2005)[3]
Northern Michigan				80-4600		40-2200	500	60-2280	3500-4550	219-355	Cadle et al. (1990)[4]
Barbados			578-869				336-409	264-315			Galloway et al. (1993)
Bermuda			560-749				273-447	182-242			Galloway et al. (1993)
Ireland			1692-5800				535-1258	321-734			Galloway et al. (1993)
Vitoria, Spain	3983		3625	1151	3030	1739	2303	2830			Encinas et al. (2004)
Central France				20000-250000		500-8500	4500-16500	750-5250			Bourcier et al. (2012)
Sardinia, Italy	3459-4605	1013-1524	1708-1815	1630-1845	2085-2419		754-1062	1728-2173			Guerzoni et al. (1995)
Turkey	1649±466		789±176	619±138		624±147	612±228	1177±301			Tuncel and Ungör (1996)
Mt. Sonnblick, Austria						2160	3120	1680			Kasper-Giebl et al. (1998)[2]
							1104	1056	3480	96	Kasper-Giebl et al. (1998)[1]
Hyderabad, India	2265	877	517	723	109	389	317	160			Kulshrestha et al. (2009)
Bay of Bengal	582	5039	5282	58	16085	336	3591	426			Kulshrestha et al. (2009)
Nepal	1805±1873	2580±2277	1393±1593	2436±2092	2582±1870	1811±2351	2502±2007	487±326			Shrestha et al. (2002)
Singapore	697±376	318±201	500±180	744±590	2624±1129	1660±1284	2134±1671	2596±2076			He and Balasubramanian (2008)
Maldives	470-1200	500	1000-1100	140-220	1100-1200	530-600	930-2000	490-580			Granat et al. (2010)

Table S5: Gas and particle scavenging ratios for nitrate and sulfate derived from multiple linear regression [C_{prec} = constant + $W_{gas}C_{gas,air}$ + $W_{part}C_{part,air}$]. C_{prec} is the total precipitation concentration of nitrate or sulfate; W_{gas} and W_{part} are the gas and particle scavenging ratios, respectively; $C_{gas,air}$ and $C_{part,air}$ are the air concentrations of HNO_3 or SO_2 and pNO_3^- or pSO_4^{2-}, respectively. R^2 is the coefficient of determination and r-part is the partial correlation. ns indicates not significant coefficients (p>0.05).

Site	W_{pNO3}	W_{HNO3}	R^2	r-part pNO_3^-	r-part HNO_3		W_{pSO4}	W_{SO2}	R^2	r-part pSO_4^{2-}	r-part SO_2
Saturna	910	1175	0.20	0.22	0.33		903	45	0.14	0.31	0.06
Bratt's Lake	694	1359	0.16	0.29	0.25				<0.1		
Algoma	1121	1253	0.24	0.25	0.28		434	85	0.17	0.33	0.08
Longwoods	544	776	0.14	0.28	0.21		393	ns	0.12	0.33	-0.01
Egbert	523	722	0.18	0.30	0.20		391	ns	0.16	0.37	0.01
Sprucedale	882	1308	0.21	0.21	0.26		505	ns	0.13	0.35	-0.02
Chalk River	786	1510	0.17	0.15	0.28		487	ns	0.14	0.36	-0.01
Chapais	1776	2848	0.25	0.16	0.39		623	409	0.20	0.41	-0.04
Sutton	944	1241	0.15	0.19	0.25		535	31	0.17	0.39	0.03
Lac Edouard	1532	1289	0.33	0.25	0.22		482	80	0.19	0.37	0.06
Frelighsburg	958	1470	0.26	0.28	0.29		526	104	0.13	0.32	0.08
Montmorency	1470	1493	0.34	0.16	0.45		481	ns	0.22	0.46	-0.03
Kejimkujik	1561	2382	0.19	0.22	0.33				<0.1		
Overall	570	1253	0.21	0.22	0.29		489	32	0.20	0.38	0.04

Table S6: Monthly gas and particle scavenging ratios for nitrate and sulfate derived from multiple linear regression (similar to Table S5)

Month	W_{pNO3}	W_{HNO3}	R^2	r-part pNO_3^-	r-part HNO_3		W_{pSO4}	W_{SO2}	R^2	r-part pSO_4^{2-}	r-part SO_2
Jan	425	1871	0.23	0.16	0.37		851	ns	0.25	0.40	-0.06
Feb	548	1511	0.27	0.24	0.35		467	184	0.20	0.34	0.00
Mar	583	1283	0.26	0.26	0.31		633	ns	0.18	0.32	0.02
Apr	442	1518	0.21	0.18	0.30		525	195	0.22	0.28	0.09
May	270	1332	0.18	0.10	0.31		434	257	0.19	0.22	0.13
Jun	373	1093	0.22	0.11	0.31		284	307	0.22	0.22	0.17
Jul	636	1005	0.19	0.13	0.29		317	204	0.21	0.26	0.09
Aug	894	1065	0.24	0.17	0.30		333	230	0.20	0.26	0.09
Sep	345	842	0.11	0.08	0.20		362	77	0.17	0.29	0.05
Oct	749	862	0.17	0.24	0.19		472	107	0.24	0.28	0.11
Nov	712	1543	0.20	0.28	0.24		780	21	0.21	0.35	0.03
Dec	554	1741	0.24	0.25	0.33		670	ns	0.19	0.32	0.00

References

Sutton, M. A., Reis, S., Riddick, S. N., Dragosits, U., Nemitz, E., Theobald, M. R., Tang, Y. S., Braban, C. F., Vieno, M., Dore, A. J., Mitchell, R. F., Wanless, S., Daunt, F., Fowler, D., Blackall, T. D., Milford, C., Flechard, C. R., Loubet, B., Massad, R., Cellier, P., Personne, E., Coheur, P. F., Clarisse, L., Van Damme, M., Ngadi, Y., Clerbaux, C., Skjøth, C. A., Geels, C., Hertel, O., Wichink Kruit, R. J., Pinder, R. W., Bash, J. O., Walker, J. T., Simpson, D., Horváth, L., Misselbrook, T. H., Bleeker, A., Dentener, F., and de Vries, W.: Towards a climate-dependent paradigm of ammonia emission and deposition. Philosophical Transactions of the Royal Society B: Biological Sciences, 368(1621), doi: 10.1098/rstb.2013.0166, 2013.

Yao, X. and Zhang, L.: Trends in atmospheric ammonia at urban, rural, and remote sites across North America, Atmos. Chem. Phys., 16, 11465-11475, doi:10.5194/acp-16-11465-2016, 2016.